

Is Externally Corrected Coupled Cluster Always Better than the Underlying Truncated Configuration Interaction?

Ilias Magoulas,[†] Karthik Gururangan,[†] Piotr Piecuch,^{*,†,‡} J. Emiliano Deustua,[†]
and Jun Shen[†]

[†]*Department of Chemistry, Michigan State University, East Lansing, Michigan 48824, USA*

[‡]*Department of Physics and Astronomy, Michigan State University, East Lansing,
Michigan 48824, USA*

E-mail: piecuch@chemistry.msu.edu

Abstract

The short answer to the question in the title is ‘no’. We identify classes of truncated configuration interaction (CI) wave functions for which the externally corrected coupled-cluster (ec-CC) approach using the three-body (T_3) and four-body (T_4) components of the cluster operator extracted from CI does not improve the results of the underlying CI calculations. Implications of our analysis, illustrated by numerical examples, for the ec-CC computations using truncated and selected CI methods are discussed. We also introduce a novel ec-CC approach using the T_3 and T_4 amplitudes obtained with the selected CI scheme abbreviated as CIPSI, correcting the resulting energies for the missing T_3 correlations not captured by CIPSI with the help of moment expansions similar to those employed in the completely renormalized CC methods.

1 INTRODUCTION

It is well-established that methods based on the exponential wave function ansatz^{1,2} of coupled-cluster (CC) theory,³⁻⁶

$$|\Psi\rangle = e^T|\Phi\rangle, \tag{1}$$

where

$$T = \sum_{n=1}^N T_n \tag{2}$$

is the cluster operator, T_n is the n -body component of T , N is the number of correlated electrons, and $|\Phi\rangle$ is the reference determinant defining the Fermi vacuum, are among the most efficient ways of incorporating many-electron correlation effects in molecular applications.^{7,8} However, the conventional and most practical single-reference CC methods, including the CC singles and doubles (CCSD) approach,^{9,10} where T is truncated at T_2 , and the quasi-perturbative correction to CCSD due to T_3 clusters defining the widely used CCSD(T) approximation,¹¹ fail in multi-reference situations, such as bond breaking and strongly correlated systems (cf., e.g., refs 7,8,12). In fact, no traditional truncation in the cluster operator at a given many-body rank, including higher-order CC methods, such as the CC approach with singles, doubles, and triples (CCSDT), where T is truncated at T_3 ,^{13,14} and the CC approach with singles, doubles, triples, and quadruples (CCSDTQ), where T is truncated at T_4 ,^{15,16} can handle systems with larger numbers of strongly correlated electrons.^{17,18} Since conventional multi-reference methods of quantum chemistry^{7,8,19,20} may be inapplicable to such problems as well (in part due to rapidly growing dimensionalities of the underlying active spaces), it is worth exploring various alternative ideas, including those that combine different wave function ansätze, which would allow us to provide an accurate and balanced description of nondynamic and dynamic correlations in a wide range of many-electron systems encountered in chemical applications.

One of the interesting ways of improving the results of single-reference CC calculations in multi-reference and strongly correlated situations, which is based on combining the CC and

non-CC (e.g., configuration interaction (CI)) concepts and which is the main topic of this study, is the externally corrected CC (ec-CC) framework^{21–31} (see ref 32 for a review). The ec-CC approaches are based on the observation that as long as the electronic Hamiltonian H does not contain higher-than-two-body interactions, the CC amplitude equations projected on the singly and doubly excited determinants,

$$\langle \Phi_i^a | (H_N e^T)_C | \Phi \rangle = 0 \quad (3)$$

and

$$\langle \Phi_{ij}^{ab} | (H_N e^T)_C | \Phi \rangle = 0, \quad (4)$$

respectively, in which no approximations are made, do not engage the higher-rank T_n components of the cluster operator T with $n > 4$. Thus, by solving these nonlinear, energy-independent, equations, which can also be written as

$$\begin{aligned} \langle \Phi_i^a | [F_N + (F_N T_1)_C + (F_N T_2)_C + (F_N \frac{1}{2} T_1^2)_C + (V_N T_1)_C + (V_N T_2)_C + (V_N \frac{1}{2} T_1^2)_C \\ + (V_N T_3)_C + (V_N T_1 T_2)_C + (V_N \frac{1}{3!} T_1^3)_C] | \Phi \rangle = 0, \end{aligned} \quad (5)$$

$$\begin{aligned} \langle \Phi_{ij}^{ab} | [(F_N T_2)_C + (F_N T_3)_C + (F_N T_1 T_2)_C + V_N + (V_N T_1)_C + (V_N T_2)_C + (V_N \frac{1}{2} T_1^2)_C \\ + (V_N T_3)_C + (V_N T_1 T_2)_C + (V_N \frac{1}{3!} T_1^3)_C \\ + (V_N T_4)_C + (V_N T_1 T_3)_C + (V_N \frac{1}{2} T_2^2)_C + (V_N \frac{1}{2} T_1^2 T_2)_C + (V_N \frac{1}{4!} T_1^4)_C] | \Phi \rangle = 0, \end{aligned} \quad (6)$$

for the singly and doubly excited clusters, T_1 and T_2 , respectively, in the presence of their exact triply (T_3) and quadruply (T_4) excited counterparts extracted from full CI (FCI), one obtains the exact T_1 and T_2 and the exact correlation energy $\Delta E \equiv E - \langle \Phi | H | \Phi \rangle$, which in the case of the Hamiltonians with two-body interactions is given by the expression

$$\Delta E = \langle \Phi | (H_N e^T)_{FC} | \Phi \rangle = \langle \Phi | [(F_N T_1)_{FC} + (V_N T_2)_{FC} + (V_N \frac{1}{2} T_1^2)_{FC}] | \Phi \rangle. \quad (7)$$

This suggests that by using external wave functions capable of generating an accurate representation of T_3 and T_4 clusters, and subsequently solving for T_1 and T_2 using eqs 5 and 6, one should not only produce correlation energies that are much better than those obtained with CCSD, where T_3 and T_4 are zero, but also substantially improve the results of the calculations used to provide T_3 and T_4 .

One of the two main objectives of this study is to examine the validity of the latter part of the above suggestion. By performing the appropriate mathematical analysis, backed by numerical examples, we point out that, in addition to the exact, FCI or full CC, states, there exist large classes of truncated CI and CC wave functions which, after extracting T_1 through T_4 from them via the cluster analysis procedure adopted in all ec-CC considerations, satisfy eqs 5 and 6. In all those cases, which are further elaborated on in Section 2, the ec-CC calculations return back the energies obtained in the calculations that provide T_3 and T_4 clusters. While it is obvious that any CC state with $T = \sum_{n=1}^M T_n$, where $2 \leq M \leq N$, including the conventional CCSD ($M = 2$), CCSDT ($M = 3$), CCSDTQ ($M = 4$), etc. truncations and their active-space CCSDt, CCSDtq, etc. analogs,³³ which all treat the T_1 and T_2 components of T fully, satisfies eqs 5 and 6, the finding that there are truncated CI states that result in the T_n operators with $n = 1-4$ which are solutions of eqs 5 and 6 is less trivial, while having interesting consequences for the ec-CC methods using CI wave functions to determine T_3 and T_4 . Throughout this article, we use the notation in which $|\Phi_{i_1 \dots i_n}^{a_1 \dots a_n}\rangle$ are the n -tuply excited determinants, with i, j, \dots and a, b, \dots representing the occupied and unoccupied spin-orbitals in $|\Phi\rangle$, respectively, $H_N = H - \langle \Phi | H | \Phi \rangle = F_N + V_N$ is the Hamiltonian in the normal-ordered form, with F_N and V_N representing its one- and two-body components, and $(AB)_{FC}$, $(AB)_C$, and AB are the fully connected, connected but not fully connected, and disconnected products of operators A and B , respectively. In the language of diagrams, $(AB)_{FC}$ is a connected operator product having no external fermion lines, $(AB)_C$ is a connected operator product with some fermion lines left uncontracted, and AB implies that no fermion lines connect A and B . It should be noted that the connected

operator product is not necessarily the same as a connected quantity in a diagrammatic sense of the many-body perturbation theory (MBPT), since operators A and B involved in forming $(AB)_{FC}$ or $(AB)_C$ may themselves be disconnected or, even, unlinked. For example, the T_n components of the cluster operator T , which enter eqs 5–7, are connected in a sense of MBPT diagrammatics if they originate from standard CC computations or cluster analysis of FCI, but they may no longer be connected if obtained from cluster analysis of truncated CI wave functions. The latter remark is particularly relevant to the subject of this study. The connected operator product only means that operators A and B , each treated as a whole, are connected with at least one fermion line, but the connectedness of $(AB)_C$ in the MBPT sense depends on the contents of A and B .

The formal and numerical results reported in this study may have implications for the development of future methods based on the ec-CC ideas. The external sources of T_3 and T_4 clusters adopted in the ec-CC methods developed to date include projected unrestricted Hartree–Fock wave functions, which were used in the past to rationalize diagram cancellations defining the approximate coupled-pair approaches, when applied to certain classes of strongly correlated model systems^{21,22,34} (see, also, ref 32 and references therein), and wave functions obtained with methods designed to capture nondynamic correlation effects relevant to molecular applications, such as bond breaking and polyradical species, including valence-bond,²³ complete-active-space self-consistent-field (CASSCF),^{24,25} multi-reference CI (MRCI),^{27–29} perturbatively selected CI (PSCI),²⁶ FCI quantum Monte Carlo (FCIQMC),^{30,35} and adaptive CI (ACI)³¹ approaches. One could also develop extensions of the ec-CC formalism by considering projections of the CC equations on higher–than–doubly excited determinants and extracting the relevant T_n components with $n \geq 4$ from a non-CC source, as in the ecCCSDt-CASSCF scheme of ref 36, where the authors corrected the CCSDt equations by the T_4 - and T_5 -containing terms extracted from CASSCF. While some of the above ec-CC methods, especially the reduced multi-reference CCSD (RMRCCSD) approach,^{27,28} which uses T_3 and T_4 clusters extracted from MRCI, and its RMRCCSD(T) extension correcting

the RMRCCSD energies for certain types of T_3 correlations missing in MRCI wave functions,²⁹ the PSCI-based ec-CC scheme introduced in ref 26, and the cluster-analysis-driven FCIQMC (CAD-FCIQMC) approach of refs 30,35, which utilizes T_3 and T_4 amplitudes extracted from stochastic wave function propagations defining the FCIQMC framework,^{37–40} offer considerable improvements compared to both CCSD and the underlying CI calculations providing T_3 and T_4 clusters (cf., e.g., refs 27–29,41–46 for illustrative examples of successful RMRCC computations), there are situations where the improvements are minimal or none.

The most recent example demonstrating that the ec-CC computations do not necessarily outperform the underlying CI calculations is the ACI-CC method implemented in ref 31. In the ACI-CC method, which we suggested two years earlier,³⁰ but have not followed through, one uses T_3 and T_4 clusters extracted from the wave functions obtained with the ACI approach.^{47,48} As shown, for example, in Table 2 of ref 31, the ACI-CCSD calculations worsen the underlying ACI results for the automerization of cyclobutadiene so much that there is virtually no difference between the ACI-CCSD and poor CCSD energetics (see, also, Figure 5 in ref 31). The enrichment of the ACI wave functions using MRCI-like arguments through the extended ACI approach abbreviated by the authors of ref 31 as xACI, followed by cluster analysis to obtain T_3 and T_4 and ec-CC iterations to determine T_1 and T_2 , defining the xACI-CCSD method, improves the ACI-CCSD barrier heights, but the xACI-CCSD computations do not improve the corresponding ACI and xACI results. Similar remarks apply to the potential energy curve and vibrational term values of the beryllium dimer, shown in Figure 2 and Table 1 of ref 31, where there is virtually no difference between the CCSD(T) and ACI-CCSD(T) data (ACI-CCSD(T) stands for the ACI-CCSD calculations corrected for the T_3 correlations missing in the ACI wave functions). This shows that there are classes of truncated CI wave functions that are either good enough in their own right or that have a specific mathematical structure such that the ec-CC calculations using them do not offer any significant benefits, while adding to the computational costs.

This leads us to the second objective of the present study, discussed mostly in Section 3,

namely, the exploration of an alternative to ACI, abbreviated as CIPSI, which stands for the CI method using perturbative selection made iteratively,^{49–51} as a source of T_3 and T_4 clusters in the ec-CC considerations. In analogy to ACI, CIPSI belongs to the broader category of selected CI approaches, which date back to the late 1960s and early 1970s^{49,52–54} and which have recently attracted renewed attention.^{47,48,50,51,55–61} In addition to using CIPSI to support parts of our mathematical analysis presented in Section 2, we demonstrate that the ec-CC approach using T_3 and T_4 cluster components extracted from the CIPSI wave functions improves the underlying CIPSI results, especially after correcting the ec-CC energies for the missing T_3 correlations. On the other hand, as further discussed in Section 3, the energies obtained with CIPSI corrected using multi-reference second-order MBPT can be competitive with the corresponding CIPSI-driven ec-CC computations, at least when smaller molecular systems are examined. This agrees with the excellent performance of the perturbatively corrected CIPSI approach, when compared with other methods aimed at near-FCI energetics, including the ec-CC-based CAD-FCIQMC scheme, observed, for example, in ref 62, which reinforces the importance of the question posed in the title of this work.

2 CLASSES OF CI WAVE FUNCTIONS THAT SATISFY ec-CC EQUATIONS

We begin our considerations with the formal analysis, supported by the numerical evidence shown in Tables 1–3, aimed at identifying the non-exact ground-state wave functions $|\Psi\rangle$ that, after performing cluster analysis on them, result in the T_1 through T_4 components satisfying eqs 5 and 6 and returning back the energies associated with these $|\Psi\rangle$ states. The mathematics of the ec-CC framework, focusing on the ec-CC approaches using truncated CI wave functions to generate T_3 and T_4 clusters, and its implications are discussed in Section 2.1. The calculations illustrating the ec-CC theory aspects examined in Section 2.1 are discussed in Section 2.2.

2.1 Mathematical Analysis of the ec-CC Formalism

We have already noted that any state resulting from the CC calculations using $T = \sum_{n=1}^M T_n$, where $2 \leq M \leq N$, starting with the basic CCSD approximation and including the remaining members of the conventional CCSD, CCSDT, CCSDTQ, etc. hierarchy, satisfies eqs 5 and 6. In fact, any wave function $|\Psi\rangle$ that uses the exponential CC ansatz defined by eq 1 and treats T_1 and T_2 clusters fully satisfies these equations too. This alone, while obvious to CC practitioners, might already be a potential issue in the context of ec-CC considerations, since, at least in principle, one can envision situations where some non-exact, non-CC approaches recreate, to a good approximation, such CC states and energies associated with them, diminishing the value of the corresponding ec-CC calculations.

As elaborated on in this subsection, and as demonstrated in Appendices A and B which contain the relevant mathematical proofs, similar statements apply to certain classes of truncated CI approaches, when used as providers of T_3 and T_4 clusters for ec-CC computations. In particular, if we use any conventional CI truncation to define the ground state $|\Psi\rangle$ in which singly and doubly excited contributions are treated fully, as in the CISD, CISDT, CISDTQ, etc. approaches, i.e.,

$$|\Psi\rangle = (1 + C)|\Phi\rangle, \quad (8)$$

where we assumed the intermediate normalization and where

$$C = \sum_{n=1}^M C_n \quad (9)$$

is the corresponding excitation operator, with C_n representing its n -body components and $2 \leq M \leq N$, and then, after determining the CI excitation amplitudes by diagonalizing the Hamiltonian, define the cluster operator T as

$$T = \ln(1 + C) = \sum_{m=1}^N \frac{(-1)^{m-1}}{m} C^m, \quad (10)$$

to bring the CI expansion, eq 8, to an exponential form, eq 1, which leads to the well-known definitions of the T_1 through T_4 components adopted in all ec-CC methods,

$$\begin{aligned}
T_1 &= C_1, \\
T_2 &= C_2 - \frac{1}{2}C_1^2, \\
T_3 &= C_3 - C_1C_2 + \frac{1}{3}C_1^3, \\
T_4 &= C_4 - C_1C_3 - \frac{1}{2}C_2^2 + C_1^2C_2 - \frac{1}{4}C_1^4,
\end{aligned}
\tag{11}$$

the resulting T_n , $n = 1-4$, amplitudes satisfy eqs 5 and 6. In other words, if we extract the T_3 and T_4 components of T through the cluster analysis of the CI state $|\Psi\rangle$ defined by eqs 8 and 9, using the relationships between the C_n and T_n operators given by eq 11, and solve for T_1 and T_2 in the presence of T_3 and T_4 obtained in this way, we recover the truncated CI energy associated with $|\Psi\rangle$ back, without improving it at all. This means that if we follow the above recipe, without making any additional *a posteriori* modifications in T_3 and T_4 , which we refer to as variant I of ec-CC, abbreviated throughout this paper as ec-CC-I, the ec-CC calculations using the CISD, CISDT, CISDTQ, etc. wave functions to generate T_3 and T_4 with the help of eq 11 reproduce the corresponding CI energies, nothing more. At first glance, the ec-CC-I calculations using the CISD and CISDT states as external sources of T_3 and T_4 amplitudes seem strange, but, as further clarified by the proofs presented in Appendices A and B, there is nothing strange about it. If we do not impose any constraints on the T_3 and T_4 components resulting from the cluster analysis defined by eq 11, the ec-CC calculations using the CISD or CISDT wave functions are as legitimate as all others. The unconstrained ec-CC-I calculations using the CISD and CISDT wave functions in a cluster analysis return back the corresponding CISD and CISDT energies, since the ec-CC-I scheme, as summarized above, allows for the purely disconnected T_3 and T_4 amplitudes, such as

$$T_3 = -C_1C_2 + \frac{1}{3}C_1^3 \tag{12}$$

or

$$T_4 = -C_1C_3 - \frac{1}{2}C_2^2 + C_1^2C_2 - \frac{1}{4}C_1^4. \quad (13)$$

This undesirable feature of the ec-CC-I scheme is a consequence of artificially imposing the exponential structure of the wave function on a truncated CI expansion, which does not have it. The only conventional CI state that can be represented by the connected T_n components by exploiting the relations between the C_n and T_n operators given by eq 11 is a FCI state.

In reality, the ec-CC-I scheme, as defined above, is never used in the context of ec-CC calculations based on T_3 and T_4 extracted from truncated CI, since allowing the purely disconnected forms of T_3 and T_4 operators, when the corresponding C_3 and C_4 amplitudes are zero, as in eqs 12 and 13, is problematic (we recall that in the exact, FCI, description, all many-body components of the cluster operator T are connected^{1,2}). To eliminate the risk of introducing the purely disconnected three- and four-body components of the cluster operator T into the ec-CC equations for T_1 and T_2 , eqs 5 and 6, in all practical implementations of the ec-CC methodology employing truncated CI wave functions, such as those reported in refs 26–29,31, one keeps only those T_3 and T_4 amplitudes resulting from the cluster analysis for which the corresponding C_3 and C_4 excitation coefficients are nonzero.²⁷ This does not guarantee a complete elimination of disconnected diagrams from the resulting T_3 and T_4 amplitudes, since all Hamiltonian diagonalizations using conventional CI truncations result in unlinked wave function contributions that do not cancel out, but it does take care of the negative consequences associated with the presence of the purely disconnected T_3 and T_4 terms that fall into the category of expressions represented by eqs 12 and 13. The resulting ec-CC protocol, in which one does not allow the problematic T_3 and T_4 components that do not have the companion C_3 and C_4 amplitudes, is called in this paper variant II of ec-CC, abbreviated as ec-CC-II. The RMRCCSD approach introduced in ref 27, the ACI-CCSD scheme implemented in ref 31, and the CIPSI-driven ec-CC-II algorithm discussed in Section 3 are the examples of ec-CC methods in this category. The removal of certain classes of triples and quadruples from the ec-CC considerations, which results from imposing the

above constraint on the T_3 and T_4 amplitudes allowed in eqs 5 and 6, can be compensated by correcting the ec-CC-II energies for the missing T_3 or T_3 and T_4 correlations, as in the CCSD(T)-like triples corrections to RMRCCSD and ACI-CCSD adopted in refs 29 and 31, defining the RMRCCSD(T) and ACI-CCSD(T) approaches, respectively, and the CIPSI-based ec-CC-II₃ method introduced in Section 3, which relies on the more accurate moment corrections. We will return to the issue of correcting the ec-CC-II energies for the missing T_3 correlations when discussing our new CIPSI-driven ec-CC-II approach in the next section.

The ec-CC-II protocol eliminates problems resulting from allowing the purely disconnected forms of T_3 and T_4 operators in the ec-CC calculations, when the corresponding C_3 and C_4 amplitudes are zero, but it does not prevent the collapse of the ec-CC energies onto their CI counterparts. The ec-CC-II computations, in which the T_3 and T_4 clusters entering eqs 5 and 6 are extracted from CI calculations using a complete treatment of singles, doubles, triples, and quadruples, as in the CISDTQ, CISDTQP, CISDTQPH, etc. truncations, where M in eq 9 is at least 4 and letters ‘P’ and ‘H’ in the CISDTQP and CISDTQPH acronyms stand for pentuples (C_5) and hexuples (C_6), respectively, return back the corresponding CI energies. In all of these cases, the ec-CC methodology, including even its most proper ec-CC-II variant, offers no benefits whatsoever, while adding to the computational costs associated with cluster analysis of the underlying CI wave functions and dealing with eqs 5 and 6 after the respective CI Hamiltonian diagonalizations. This is because once all singles, doubles, triples, and quadruples are included in CI calculations, every nonzero T_n , $n = 3, 4$, amplitude resulting from the cluster analysis of the underlying CI state has a companion, also nonzero, C_n excitation coefficient, i.e., the ec-CC-I and ec-CC-II schemes become equivalent. One might argue that the above observation does not diminish the usefulness of ec-CC computations, since one never uses high-level single-reference CI methods, such as CISDTQ, as sources of T_3 and T_4 amplitudes in practical applications, which is a correct statement, but a remark like that could be misleading. Nowadays, one can generate approximate CI-type wave functions that provide a highly accurate representation of the C_n

components through quadruples and beyond in computationally efficient ways via stochastic CIQMC propagations^{37–40} and semi-stochastic implementations of selected CI techniques, as in heat-bath CI^{59–61} and modern implementations of CIPSI.^{50,51} As shown in Section 3, the ec-CC-II₃ approach using the T_3 and T_4 clusters extracted from the CIPSI wave functions and corrected for the missing T_3 correlations does not have to improve the corresponding CIPSI energetics corrected using second-order MBPT when smaller many-electron problems are examined.

If we limit ourselves to conventional CI truncations defined by eqs 8 and 9, the only situations where the ec-CC-I and ec-CC-II protocols differ, giving the ec-CC-II approach a chance to improve the results of the corresponding ec-CC-I and CI computations, are those in which T_3 and T_4 clusters are extracted from CISD or CISDT. To be more specific, when one uses the CISD wave function, where C_3 and C_4 are by definition zero, in the ec-CC-II calculations, which means that T_3 and T_4 in eqs 5 and 6 are set at zero as well, the ec-CC-II energy becomes equivalent to that obtained with CCSD, as opposed to the usually less accurate CISD value obtained with ec-CC-I. When the CISDT wave function is employed in the ec-CC-II computations, one solves eqs 5 and 6 for T_1 and T_2 in the presence of T_3 contributions having companion C_3 excitation amplitudes extracted from CISDT, which may lead to major improvements compared to the corresponding ec-CC-I calculations that return back the CISDT energy and the results obtained with CCSD, in which T_3 is ignored, but since $C_4 = 0$ in CISDT, i.e., T_4 correlations are not accounted for, the CISDT-based ec-CC-II approach may produce erratic results in more complex multi-reference situations. We will return to the discussion of these accuracy patterns, including the equivalence of the ec-CC-I, ec-CC-II, and the underlying CI approaches when the ec-CC calculations use wave functions characterized by a full treatment of C_n amplitudes with $n = 1–4$, during the examination of the numerical results shown in Table 1 in Section 2.2.

As shown in Appendices A and B, the above relationships between the results of the ec-CC calculations using T_3 and T_4 clusters extracted from truncated CI computations and the

corresponding CI energetics can be generalized to unconventional truncations in the linear excitation operator C defining the wave function $|\Psi\rangle$ via eq 8 as long as the C_1 and C_2 components of C contain a complete set of singles and doubles. To state this generalization, which is the heart of the mathematical and numerical analysis presented in this section, more precisely, let us consider the CI eigenvalue problem in which the ground electronic state is defined as follows:

$$|\Psi\rangle = (1 + C^{(P_A)} + C^{(P_B)}) |\Phi\rangle, \quad (14)$$

where the singly and doubly excited components of $|\Psi\rangle$, described by the $C^{(P_A)}$ operator, are treated fully, i.e.,

$$C^{(P_A)} = C_1 + C_2, \quad (15)$$

and where the remaining wave function contributions, if any, are represented by

$$C^{(P_B)} = \sum_{n \geq 3} C_n^{(P_B)} \quad (16)$$

(as in the case of eq 8, we impose the intermediate normalization on $|\Psi\rangle$). We do not make any specific assumptions regarding the $C^{(P_B)}$ operator other than the requirement that it does not contain the one- and two-body components of C , which are included in $C^{(P_A)}$. The above definitions encompass the previously discussed conventional CI truncations, starting from CISD, where $C^{(P_B)} = 0$, and including the remaining members of the CISD, CISDT, CISDTQ, etc. hierarchy, for which the relevant n -body components of $C^{(P_B)}$ are treated fully, and the various selected CI approaches with all singles and doubles and subsets of higher-than-double excitations. To facilitate our discussion below, and to aid the presentation of the proofs in Appendices A and B, we designate the subspace of the many-electron Hilbert space \mathcal{H} spanned by the singly and doubly excited determinants, $|\Phi_i^a\rangle$ and $|\Phi_{ij}^{ab}\rangle$, respectively, which are jointly abbreviated as $|\Phi_\alpha\rangle$ and which match the content of the $C^{(P_A)}$ operator defined by eq 15, as $\mathcal{H}^{(P_A)}$. The subspace of \mathcal{H} spanned by the determinants corresponding

to the content of $C^{(P_B)}$, eq 16, denoted as $|\Phi_\beta\rangle$, is designated as $\mathcal{H}^{(P_B)}$, and the orthogonal complement to $\mathcal{H}^{(P)} \oplus \mathcal{H}^{(P_A)} \oplus \mathcal{H}^{(P_B)}$, which contains the remaining determinants $|\Phi_\gamma\rangle$ not included in the CI wave function $|\Psi\rangle$, is denoted as $\mathcal{H}^{(Q)}$ ($\mathcal{H}^{(P)}$ is a one-dimensional subspace of \mathcal{H} spanned by the reference determinant $|\Phi\rangle$). Using the above notation, we can write the CI eigenvalue problem for the ground-state wave function $|\Psi\rangle$ given by eq 14 and the corresponding correlation energy $\Delta E^{(CI)}$ as follows:

$$\langle\Phi_\alpha|H_N(1 + C^{(P_A)} + C^{(P_B)})|\Phi\rangle = \Delta E^{(CI)} \langle\Phi_\alpha|C^{(P_A)}|\Phi\rangle, \quad (17)$$

$$\langle\Phi_\beta|H_N(1 + C^{(P_A)} + C^{(P_B)})|\Phi\rangle = \Delta E^{(CI)} \langle\Phi_\beta|C^{(P_B)}|\Phi\rangle, \quad (18)$$

where $|\Phi_\alpha\rangle \in \mathcal{H}^{(P_A)}$, $|\Phi_\beta\rangle \in \mathcal{H}^{(P_B)}$, and

$$\Delta E^{(CI)} = \langle\Phi|H_N(1 + C^{(P_A)} + C^{(P_B)})|\Phi\rangle \quad (19)$$

(in the case of CISD calculations, where $C^{(P_B)} = 0$ and the set of determinants $|\Phi_\beta\rangle$ is empty, we only have to write eqs 17 and 19).

The main theorem of this work states that the ec-CC-I calculations, in which we obtain the T_3 and T_4 components entering eqs 5 and 6 by defining the cluster operator T as

$$T = \ln(1 + C^{(P_A)} + C^{(P_B)}) \quad (20)$$

and then solve eqs 5 and 6 for the T_1 and T_2 clusters in the presence of T_3 and T_4 extracted from the CI state $|\Psi\rangle$, eq 14, determined by using eqs 17–19, without eliminating any T_3 and T_4 amplitudes resulting from the cluster analysis of $|\Psi\rangle$, return back the CI correlation energy $\Delta E^{(CI)}$, eq 19, independent of truncations in $C^{(P_B)}$. In order to prove this theorem, we have to focus on the subset of CI equations represented by eq 17, which corresponds to

projections on the singly and doubly excited determinants,

$$\langle \Phi_i^a | H_N (1 + C_1 + C_2 + C^{(P_B)}) | \Phi \rangle = \Delta E^{(\text{CI})} \langle \Phi_i^a | C_1 | \Phi \rangle \quad (21)$$

and

$$\langle \Phi_{ij}^{ab} | H_N (1 + C_1 + C_2 + C^{(P_B)}) | \Phi \rangle = \Delta E^{(\text{CI})} \langle \Phi_{ij}^{ab} | C_2 | \Phi \rangle, \quad (22)$$

respectively, and the energy formula, eq 19, which, given the absence of higher-than-two-body interactions in the electronic Hamiltonian and the use of normal ordering in H_N , can also be written as

$$\Delta E^{(\text{CI})} = \langle \Phi | H_N (C_1 + C_2) | \Phi \rangle. \quad (23)$$

As demonstrated, in two different ways, in Appendices A and B, the subsystem of CI equations represented by eq 17 or eqs 21 and 22, with the correlation energy $\Delta E^{(\text{CI})}$ given by eq 19 or 23 and the cluster operator T defined by eq 20, so that the T_n components with $n = 1-4$ are obtained using eq 11, is equivalent to the CC amplitude equations projected on singles and doubles, represented by eqs 3 and 4 or, more explicitly, 5 and 6. In the proofs of this equivalence, the CI correlation energy $\Delta E^{(\text{CI})}$, eq 19 or 23, becomes the corresponding CC energy given by eq 7. The first proof of the above statement, presented in Appendix A, uses the formal definition of T , eq 20, which brings the CI expansion, eq 14, to a CC-like form given by eq 1, the well-known property of the exponential ansatz that reads (cf., e.g., refs 4,5,7,63–66)

$$H_N e^T | \Phi \rangle = e^T (H_N e^T)_C | \Phi \rangle, \quad (24)$$

and the resolution of the identity in the many-electron Hilbert space,

$$P + P_A + P_B + Q = \mathbf{1}, \quad (25)$$

where

$$P = |\Phi\rangle\langle\Phi|, \quad (26)$$

$$P_A = \sum_{\alpha'} |\Phi_{\alpha'}\rangle\langle\Phi_{\alpha'}|, \quad (27)$$

$$P_B = \sum_{\beta} |\Phi_{\beta}\rangle\langle\Phi_{\beta}|, \quad (28)$$

and

$$Q = \sum_{\gamma} |\Phi_{\gamma}\rangle\langle\Phi_{\gamma}| \quad (29)$$

are the projection operators on the aforementioned $\mathcal{H}^{(P)}$, $\mathcal{H}^{(P_A)}$, $\mathcal{H}^{(P_B)}$, and $\mathcal{H}^{(Q)}$ subspaces and $\mathbf{1}$ is the unit operator, to convert the CI eqs 17 and 19 to the CC form represented by eqs 3, 4, and 7 (or 5–7). The second proof, shown in Appendix B, which relies on a diagrammatic approach, follows the opposite direction. It starts from the CC amplitude equations projected on the singly and doubly excited determinants, eqs 5 and 6, and the associated correlation energy formula, eq 7, which are subsequently transformed into the corresponding CI amplitude and energy equations, eqs 21–23, after expressing the T_n components of T with $n = 1$ –4 in terms of the corresponding CI excitation operators C_1 , C_2 , and $C_n^{(P_B)}$, $n = 3, 4$, using eq 11.

In analogy to the previously discussed case of conventional CI truncations at a given many-body rank in the excitation operator C , defined by eqs 8 and 9, the relationship between the ec-CC calculations based on the more general form of the wave function $|\Psi\rangle$ defined by eq 14, which encompasses a wide variety of CI approximations outside the CISD, CISDT, CISDTQ, etc. hierarchy, and the underlying CI computations, as summarized above, has several implications. The most apparent one is the observation that the ec-CC-I calculations based on solving eqs 5 and 6, in which the T_3 and T_4 components of T are obtained by cluster analysis of the CI wave functions that describe singles and doubles fully and higher-than-double excitations in a partial manner, return back the underlying CI energies, without any improvements, if the purely disconnected T_3 and T_4 amplitudes of the type of eqs 12 and 13,

for which the corresponding $C_3^{(P_B)}$ and $C_4^{(P_B)}$ contributions are zero, are not eliminated. More importantly, the ec-CC-II approach, which is what one normally uses in the CI-based ec-CC computations, in which such purely disconnected T_3 and T_4 amplitudes are disregarded when setting up eqs 5 and 6, may offer improvements over the corresponding CI calculations, but only if the triply and quadruply excited manifolds considered in CI are incomplete, i.e., the $C_3^{(P_B)}$ and $C_4^{(P_B)}$ components of $|\Psi\rangle$ include fractions of triples and quadruples. Once the $C_3^{(P_B)}$ and $C_4^{(P_B)}$ operators capture all triples and quadruples (which in practice may mean their significant fractions), the ec-CC-I and ec-CC-II schemes based on the wave functions $|\Psi\rangle$ defined by eq 14 become equivalent and the resulting ec-CC energies become identical (with the large fractions of triples and quadruples, similar) to those obtained with CI. In other words, assuming that singles and doubles are treated in CI fully, one might say that the ec-CC approach improves the energies obtained in the underlying CI calculations only if the treatment of triples and quadruples in the latter calculations is incomplete. In that case, after performing the ec-CC-II computations using subsets of triples and quadruples provided by CI and selecting the T_3 and T_4 amplitudes accordingly, to match these subsets, one can obtain the desired improvements over the corresponding CI calculations, improving the CCSD energetics at the same time. This is especially true when the ec-CC-II energies are corrected for the remaining T_3 (ideally, T_3 and T_4) correlations, as in the aforementioned RMRCCSD(T) method and the CIPSI-driven ec-CC-II₃ approach discussed in Section 3. On the other hand, as mentioned in the Introduction, and as already alluded to above, the benefits offered by the CI-based ec-CC calculations compared to modern variants of selected CI techniques, represented in this work by the semi-stochastic CIPSI approach described in refs 50,51 or the ACI scheme of refs 47,48 used in the recently implemented ACI-CCSD and ACI-CCSD(T) approaches, may not be as substantial as desired.

Before discussing the numerical evidence supporting the key aspects of the above mathematical analysis in Section 2.2, it is worth mentioning that while in this study we focus on the most popular form of the ec-CC formalism, in which one solves the CC equations projected

on singles and doubles, eqs 3 and 4 or 5 and 6, for the T_1 and T_2 clusters in the presence of T_3 and T_4 extracted from the external, non-CC source, one can extend our considerations to higher-order ec-CC variants that solve for higher-than-two-body components of the cluster operator T (see, e.g., the ecCCSDt-CASSCF approach, discussed in ref 36, for an example of such a higher-order ec-CC method). This can be done by reusing eqs 17–19 and redefining subspaces $\mathcal{H}^{(P_A)}$ and $\mathcal{H}^{(P_B)}$ and the corresponding excitation operators $C^{(P_A)}$ and $C^{(P_B)}$ that enter the CI wave function $|\Psi\rangle$ through eq 14. To illustrate this, let us consider the CI eigenvalue problem in which

$$C^{(P_A)} = \sum_{n=1}^{m_A} C_n, \quad (30)$$

with $m_A \geq 2$, so that the corresponding subspace $\mathcal{H}^{(P_A)}$ is spanned by all determinants $|\Phi_\alpha\rangle$ with the excitation ranks ranging from 1 to m_A , and

$$C^{(P_B)} = \sum_{n \geq m_A+1} C_n^{(P_B)}, \quad (31)$$

where the many-body components $C_n^{(P_B)}$ with $n \geq m_A + 1$ describe contributions from the remaining determinants included in the CI calculations, designated as $|\Phi_\beta\rangle$ and spanning subspace $\mathcal{H}^{(P_B)}$. As demonstrated in Appendix A, the ec-CC-I calculations, in which one solves the CC system

$$\langle \Phi_\alpha | (H_N e^T)_C | \Phi \rangle = 0, \quad (32)$$

where $|\Phi_\alpha\rangle \in \mathcal{H}^{(P_A)}$, for the T_n components of T with $n = 1, \dots, m_A$ in the presence of the T_{m_A+1} and T_{m_A+2} clusters extracted from the CI state $|\Psi\rangle$ determined by using eqs 17–19, without eliminating any T_{m_A+1} and T_{m_A+2} amplitudes resulting from the cluster analysis of $|\Psi\rangle$, return back the CI correlation energy $\Delta E^{(CI)}$, eq 19. The ec-CC-II approach, where the purely disconnected T_{m_A+1} and T_{m_A+2} amplitudes of the type of eqs 12 and 13, for which the corresponding CI excitation coefficients in $C_{m_A+1}^{(P_B)}$ and $C_{m_A+2}^{(P_B)}$ are zero, are disregarded when setting up the CC system represented by eq 32, may improve the energies obtained in

the CI calculations used to determine T_{m_A+1} and T_{m_A+2} , but only if the excitation manifolds defining $C_{m_A+1}^{(P_B)}$ and $C_{m_A+2}^{(P_B)}$ are not treated fully. Once all n -tuply excited determinants with $n = m_A + 1$ and $m_A + 2$ are captured by the $C_{m_A+1}^{(P_B)}$ and $C_{m_A+2}^{(P_B)}$ operators, the ec-CC-I and ec-CC-II schemes based on the wave functions $|\Psi\rangle$ defined by eq 14 become equivalent and the resulting ec-CC energies become identical to those obtained with CI. In making the above statements, we took advantage of the fact that the T_n clusters with $n > m_A + 2$ do not enter eq 32, since electronic Hamiltonians do not contain higher-than-two-body interactions and the excitation ranks of determinants $|\Phi_\alpha\rangle$ do not exceed m_A .

2.2 Numerical Analysis of the ec-CC-I and ec-CC-II Schemes

The validity of the mathematical considerations discussed in Section 2.1 and Appendices A and B, and of the above remarks about the anticipated accuracy patterns in the ec-CC and the underlying CI computations, are supported by the numerical data shown in Tables 1–3. Our numerical example is the C_{2v} -symmetric double bond dissociation of the water molecule, as described by the cc-pVDZ basis set,⁶⁷ in which both O–H bonds are simultaneously stretched without changing the $\angle(\text{H–O–H})$ angle. In addition to the equilibrium geometry, designated as $R = R_e$, we considered two stretches of the O–H bonds, by factors of 2 and 3, designated in our tables as $R = 2R_e$ and $3R_e$, respectively. All three geometries adopted in our calculations were taken from ref 68. Following ref 68, in all of the post-SCF computations reported in this work, we correlated all electrons and the spherical components of d functions contained in the cc-pVDZ basis were employed throughout. In all of the CI, CC, and ec-CC computations carried out in this study, we used the restricted Hartree–Fock (RHF) determinant as a reference $|\Phi\rangle$.

We use the $\text{H}_2\text{O}/\text{cc-pVDZ}$ system as our molecular example, since it is small enough to allow all kinds of CI and CC computations, including high-level methods, such as CISDTQ and beyond⁶⁸ and CCSDTQ,^{68–70} as well as FCI,⁶⁸ which are all critical for the analysis of the ec-CC formalism presented in this work. At the same time, the C_{2v} -symmetric double bond

dissociation of the water molecule creates significant challenges to many quantum chemistry approaches. In particular, the stretched nuclear geometries considered in this study are characterized by substantial multi-reference correlation effects, which result in large triply and quadruply excited CI and CC amplitudes when a single-reference framework is employed, and which require a well-balanced description of nondynamic and dynamic correlations (see, e.g., refs 68,69). As shown, for example, in Table 1, the CISDTQ approach, which is very accurate at $R = R_e$, recovering the FCI energy to within a small fraction of a millihartree, struggles when the stretched geometries are considered, increasing the errors relative to FCI to 5.819 and 16.150 millihartree at $R = 2R_e$ and $3R_e$, respectively. The $R = 3R_e$ geometry is so demanding that even the CCSDTQ method, which is virtually exact at $R = R_e$ and $2R_e$, faces a challenge, producing the sizable -4.733 millihartree error relative to FCI when the RHF reference determinant is employed. CCSDTQ improves the erratic behavior of the CCSDT approach at $R = 3R_e$, which produces the energy 40.126 millihartree below FCI, but is not sufficient if one aims at a highly accurate description, pointing to the significance of higher-than-quadruply excited clusters in this case. A similar remark applies to the CI computations, which require an explicit inclusion of six-fold excitations if we are to recover the FCI energetics to within a millihartree at all three geometries of water considered in this study (as can be seen in Table 1, errors in the CISDTQP energies relative to FCI at $R = 2R_e$ and $3R_e$ exceed 2 and 6 millihartree, respectively).

In performing the various ec-CC computations reported in Tables 1–3, we relied on our in-house CC and cluster analysis codes, interfaced with the RHF, restricted open-shell Hartree–Fock, and integral routines in the GAMESS package.^{71,72} The CISD, CISDT, CISDTQ, CISDTQP, and CISDTQPH wave functions, which formed the non-CC sources of the three- and four-body clusters for the subsequent ec-CC-I and ec-CC-II calculations based on conventional CI truncations, presented in Table 1, were obtained using the occupation restricted multiple active space determinantal CI (ORMAS) code^{73,74} available in GAMESS. The selected CI wave functions used to provide the T_3 and T_4 cluster components for the

ec-CC-I, ec-CC-II, and ec-CC-II₃ computations based on the CIPSI methodology, shown in Tables 2 and 3, which are further elaborated on in Section 3, were determined with the Quantum Package 2.0 software.^{50,51} As in the case of other post-SCF calculations reported in this study, all of our CIPSI runs relied on the transformed one- and two-electron integrals in an RHF molecular orbital basis generated with GAMESS. While the authors of ref 68 obtained the FCI/cc-pVDZ energies of the water molecule at $R = R_e$, $2R_e$, and $3R_e$, we recalculated them in this study using the GAMESS determinantal FCI routines,⁷³⁻⁷⁵ since the FCI results at the latter two geometries reported in ref 68 were not converged tightly enough. The CCSD, CCSDT, and CCSDTQ energies were taken from ref 69, although we recalculated them here as well using our in-house CC codes interfaced with GAMESS.

As shown in Table 1, and in agreement with our mathematical analysis in Section 2.1 and Appendices A and B, the ec-CC-I energies obtained by solving eqs 5 and 6 for the singly and doubly excited clusters in the presence of the T_3 and T_4 components extracted from the CISD, CISDT, CISDTQ, CISDTQP, and CISDTQPH wave functions, without making any *a posteriori* modifications in T_3 and T_4 obtained in this way, perfectly match their CI counterparts. This is happening, since all of the above CI truncations are characterized by a complete treatment of the C_1 and C_2 operators. Similar is observed in the ec-CC-I computations relying on the selected CI wave functions, obtained in this work with CIPSI, as sources of the triply and quadruply excited clusters, when the CI diagonalization spaces are large enough to capture all or nearly all singles and doubles. This can be seen in Tables 2 and 3. Indeed, when the CIPSI calculations initiated from the RHF wave functions, shown in Table 2, capture nearly all singly and doubly excited determinants at all three geometries of water considered in this study, which happens when the input dimension parameter $N_{\text{det(in)}}$ utilized by the CIPSI methodology to terminate the buildup of the CI diagonalization spaces, defined in Section 3, is 100,000 or more, the resulting ec-CC-I energies match their CIPSI counterparts to within a microhartree. When $N_{\text{det(in)}}$ is set at 100,000, the final CI diagonalization spaces, which are used to obtain the wave functions that generate the

T_3 and T_4 clusters for the ec-CC computations, contain about 200,000 $S_z = 0$ determinants of the $A_1(C_{2v})$ symmetry (see the $N_{\text{det}(\text{out})}$ values in Table 2) and the corresponding CIPSI runs capture about 94 % of all singles and 98 % of all doubles at $R = R_e$, 100 % of singles and ~ 92 % of doubles at $R = 2R_e$, and about 91 % of all singly excited and 79 % of all doubly excited determinants at $R = 3R_e$. Interestingly, the CIPSI and CIPSI-based ec-CC-I energies agree to within a millihartree when the CI diagonalization spaces contain as little as $\sim 5,000$ – $10,000$ determinants or about 50 % of all singles and doubles. This indicates that the CIPSI approach is capable of correctly identifying the dominant singly and doubly excited determinants in the early stages of the respective CI wave function buildup, so that the subsequent ec-CC-I calculations return back the energies that are similar to those obtained in the Hamiltonian diagonalizations used to determine T_3 and T_4 .

Although one does not do it in typical applications of the CIPSI approach, we also performed a numerical experiment in which the process of building up the CI diagonalization spaces in CIPSI runs was initiated from the CISD wave function. We did this for the $R = 2R_e$ geometry. In this case, each CIPSI run was forced to provide a complete treatment of the C_1 and C_2 operators, so that, based on our mathematical considerations in Section 2.1, the resulting ec-CC-I energies and their CIPSI counterparts should be identical. As shown in Table 3, they are indeed identical for all the values of the input parameter $N_{\text{det}(\text{in})}$ that permit CIPSI runs beginning with all singly and doubly excited determinants in the initial diagonalization space (in the case of the all-electron calculations for water, as described by the spherical cc-pVDZ basis set, the CISD wave function contains 3,416 $S_z = 0$ determinants of the $A_1(C_{2v})$ symmetry, so that $N_{\text{det}(\text{in})}$ must be at least 3,416).

The above relationships between ec-CC-I and CI provide useful insights, but, as already pointed out, the realistic applications of the CI-based ec-CC methodology adopt the ec-CC-II protocol, where one keeps only those T_3 and T_4 amplitudes resulting from the cluster analysis of the underlying CI wave function for which the corresponding C_3 and C_4 excitation coefficients are nonzero. The ec-CC-II algorithm takes care of the problems resulting from the

presence of the purely disconnected forms of the T_3 and T_4 clusters, such as those represented by eqs 12 and 13, which emerge when the corresponding C_3 and C_4 amplitudes are zero, but it does not prevent the collapse of the ec-CC energies onto their CI counterparts. As implied by our formal analysis, the CI-based ec-CC-II calculations are capable of improving the corresponding CI energetics, but in order for this to happen, the triply and quadruply excited manifolds included in the CI diagonalizations used to determine T_3 and T_4 must be incomplete. Otherwise, i.e., when the underlying CI computations capture all triples and quadruples, the ec-CC-I and ec-CC-II schemes become equivalent, returning back the corresponding CI energies.

We can see all of the above patterns in our tables. Indeed, as demonstrated in Table 1, variant II of the ec-CC methodology improves the CI energetics when one uses the CISD and CISDT wave functions in the corresponding cluster analyses, but once all triples and quadruples are included in CI, as in the case of the CISDTQ-, CISDTQP-, and CISDTQPH-based ec-CC-II calculations carried out in this study, the ec-CC-II and the associated CI energies do not differ. This may result in unusual and non-systematic accuracy patterns, or even in an erratic behavior of the ec-CC-II computations. For example, normally one anticipates that when the quality of the wave function improves the resulting energies improve as well, but this is not the case when we examine the CI-based ec-CC-II energies of the water molecule at the stretched $R = 2R_e$ geometry shown in Table 1. The CISD-based ec-CC-II calculation, where $C_3 = C_4 = 0$, so that the T_3 and T_4 clusters entering eqs 5 and 6 are set at zero as well, returns the energy obtained with CCSD, reducing the massive, 72.017 millihartree, error resulting from the CISD diagonalization to 22.034 millihartree. The ec-CC-II computation, in which one solves eqs 5 and 6 for T_1 and T_2 using the T_3 amplitudes extracted from the higher-rank CISDT wave function, offers further error reduction, to a 2.920 millihartree level, but the next scheme in the ec-CC-II hierarchy in Table 1, which uses a much better wave function in the cluster analysis than CISDT, by returning back the CISDTQ energy, worsens the previous CISDT-based ec-CC-II result, increasing the error by

a factor of 2. The situation at $R = 3R_e$ is even more peculiar. In this case, the replacement of the CISD wave function by its higher-level CISDT counterpart in the ec-CC-II calculations not only worsens the CISD-based ec-CC-II, i.e., CCSD energy, increasing the 10.849 millihartree unsigned error obtained with CCSD by a factor of 7, but also places the resulting energy 77.317 millihartree below FCI. By accounting for T_4 correlations, the ec-CC-II computation employing the CISDTQ wave function in the cluster analysis improves the erratic CISDT-based ec-CC-II result, but since the CISDTQ-based ec-CC-II and CISDTQ energies are identical and the CISDTQ energy, which differs from FCI by 16.150 millihartree, is rather poor, the benefits of using the ec-CC-II methodology are virtually none in this case. This points to the need for being very careful about evolving truncated CI wave functions used in the context of ec-CC computations. The CI algorithms that capture the excitation spaces through quadruples, when going from one truncation level to the next, too rapidly are not the best candidates for the ec-CC work.

Based on our formal considerations and numerical evidence, the truncated CI wave functions that are expected to benefit most from the subsequent ec-CC computations are those which attempt to probe the many-electron Hilbert space without saturating the lower-rank excitation manifolds, especially the excitations through quadruples, too early. We have seen this in our semi-stochastic CAD-FCIQMC work,^{30,35} which relies on the cluster analysis of FCIQMC wave functions, and we can see it again in Tables 2 and 3, where we examine the performance of the CIPSI-based ec-CC-II algorithm and its ec-CC-II₃ extension that corrects the ec-CC-II energies for the missing T_3 correlations that are not accounted for in CIPSI diagonalizations. The ec-CC-II and ec-CC-II₃ approaches that rely on the CIPSI wave functions to extract the information about the leading T_3 and T_4 clusters are discussed next.

3 CIPSI-DRIVEN ec-CC

The purpose of this section is to present and test a novel form of the ec-CC approach, focusing on the ec-CC-II protocol and its ec-CC-II₃ counterpart, in which the wave functions used to generate T_3 and T_4 clusters are obtained in the Hamiltonian diagonalizations defining the CIPSI approach, as implemented in the Quantum Package 2.0.^{50,51} As in the case of the numerical analysis discussed in Section 2.2, we used the water molecule, as described by the cc-pVDZ basis set, at the equilibrium and two displaced geometries in which both O–H bonds were simultaneously stretched by factors of 2 and 3 without changing the $\angle(\text{H–O–H})$ angle, to illustrate the performance of the CIPSI-driven ec-CC-II and ec-CC-II₃ methods.

We recall that, in analogy to many other selected CI schemes, the main idea of CIPSI is to perform a series of CI calculations using increasingly large, iteratively defined, diagonalization spaces, designated as \mathcal{V}_{int} . The construction of the \mathcal{V}_{int} space for a given CIPSI iteration is carried out using a perturbative selection of the singly and doubly excited determinants from the previously determined \mathcal{V}_{int} . To be more precise, if $|\Psi^{(\text{CIPSI})}\rangle = \sum_{|\Phi_I\rangle \in \mathcal{V}_{\text{int}}} c_I |\Phi_I\rangle$ is a CI wave function associated with a given CIPSI iteration, where the coefficients c_I and the corresponding energy E_{var} are obtained by diagonalizing the Hamiltonian in the current \mathcal{V}_{int} space, the diagonalization space for the subsequent CIPSI iteration is constructed using a perturbative selection of the singly and doubly excited determinants out of $|\Psi^{(\text{CIPSI})}\rangle$. Thus, if \mathcal{V}_{ext} designates the space of singly and doubly excited determinants out of $|\Psi^{(\text{CIPSI})}\rangle$, we calculate the second-order MBPT energy correction associated with each individual determinant $|\Phi_\rho\rangle \in \mathcal{V}_{\text{ext}}$, $e_\rho^{(2)} = |\langle \Phi_\rho | H | \Psi^{(\text{CIPSI})} \rangle|^2 / (E_{\text{var}} - \langle \Phi_\rho | H | \Phi_\rho \rangle)$, and use the resulting $e_\rho^{(2)}$ values to determine how to enlarge the current space \mathcal{V}_{int} . One can initiate CIPSI iterations, each consisting of the diagonalization of the Hamiltonian in the current space \mathcal{V}_{int} to determine $|\Psi^{(\text{CIPSI})}\rangle$ and the identification of the associated \mathcal{V}_{ext} space needed to construct \mathcal{V}_{int} for the subsequent iteration, by starting from a single determinant, such as the RHF wave function, or a multi-determinantal state obtained, for example, in some preliminary CI calculation.

Following refs 50,51, in the specific CIPSI model adopted in this work, used to perform the CIPSI calculations for water reported in Tables 2 and 3, the actual \mathcal{V}_{ext} spaces were obtained by stochastic sampling of the most important singles and doubles out of the $|\Psi^{(\text{CIPSI})}\rangle$ wave functions and the sampled determinants $|\Phi_\rho\rangle$ generated in each CIPSI iteration were arranged in descending order according to their $|e_\rho^{(2)}|$ values. We then enlarged each space \mathcal{V}_{int} , to be used in the subsequent CI diagonalization, starting from the determinants $|\Phi_\rho\rangle$ with the largest $|e_\rho^{(2)}|$ contributions and moving toward those with the smaller values of $|e_\rho^{(2)}|$, until the dimension of \mathcal{V}_{int} was increased by the user-defined factor f (in reality, this increase in the dimension of \mathcal{V}_{int} , from one CIPSI iteration to the next, was always slightly larger to ensure that the resulting CI wave function remained an eigenfunction of total spin). In all of the CIPSI calculations reported in this study, we set f at 2 (which is the default value of f in Quantum Package 2.0), forcing the CIPSI wave function $|\Psi^{(\text{CIPSI})}\rangle$ to grow in a tempered manner, without saturating the lower-rank excitation manifolds too rapidly, while probing the many-electron Hilbert space more effectively at the same time. To obtain the CI wave function of a given CIPSI run used to determine the T_3 and T_4 clusters employed in the ec-CC computations, we chose to terminate the sequence of CIPSI diagonalizations when the dimension of space \mathcal{V}_{int} exceeded the input parameter $N_{\text{det}(\text{in})}$. Due to the aforementioned dimension-doubling growth mechanism, the size of the CI wave function at the end of a given CIPSI calculation, denoted as $N_{\text{det}(\text{out})}$, always exceeded $N_{\text{det}(\text{in})}$, but never by more than a factor of 2.

As a byproduct of calculating energy corrections $e_\rho^{(2)}$ associated with the sampled determinants $|\Phi_\rho\rangle \in \mathcal{V}_{\text{ext}}$ generated in each CIPSI iteration, in addition to the variational energies E_{var} , one has an immediate access to the total second-order multi-reference MBPT corrections $\Delta E^{(2)} = \sum_{|\Phi_\rho\rangle \in \mathcal{V}_{\text{ext}}} e_\rho^{(2)}$. For each CIPSI run carried out in this study, as defined by the aforementioned wave function termination parameter $N_{\text{det}(\text{in})}$, we report the uncorrected energy E_{var} corresponding to the CI wave function obtained in the last Hamiltonian diagonalization of that run and its perturbatively corrected $E_{\text{var}} + \Delta E^{(2)}$ counterpart. The

determination of $\Delta E^{(2)}$ is also important for a different reason. Although the stopping criterion adopted in our CIPSI runs executed with Quantum Package 2.0 relies on the above wave function termination parameter $N_{\text{det(in)}}$, the CIPSI iterations can also stop if the magnitude of the total second-order MBPT correction $\Delta E^{(2)}$ falls below a threshold parameter η . To prevent this from happening, we used a very tight η value of 10^{-6} hartree.

After the completion of each CIPSI run, we cluster analyzed the wave function $|\Psi^{(\text{CIPSI})}\rangle$ obtained in the final Hamiltonian diagonalization of that run and used the resulting T_3 and T_4 components to perform the corresponding ec-CC computations. Since in the ec-CC-II calculations that interest us in this section the purely disconnected T_3 and T_4 amplitudes of the type of eqs 12 and 13, for which the corresponding C_3 and C_4 contributions are zero, are disregarded when setting up eqs 5 and 6, we corrected the ec-CC-II correlation energies ΔE , determined using eq 7, for the missing T_3 effects not captured by ec-CC-II. In order to do this, we adopted the formulas that we previously used to develop the deterministic^{69,76,77} and semi-stochastic^{70,78,79} CC(P ; Q) approaches. According to the biorthogonal moment expansions behind the CC(P ; Q) framework, the corrections to the ec-CC-II correlation energies ΔE due to the T_3 effects not captured by the CIPSI wave functions, subjected to the so-called two-body approximation introduced in ref 76 that has been shown to provide a highly accurate representation of these effects,^{69,76,77} can be defined as follows:

$$\delta_3 = \sum_{|\Phi_{ijk}^{abc}\rangle \notin \mathcal{V}_{\text{int}}} \varrho_{ijk}^{abc}(2) \mathfrak{M}_{abc}^{ijk}(2). \quad (33)$$

Here,

$$\mathfrak{M}_{abc}^{ijk}(2) = \langle \Phi_{ijk}^{abc} | \overline{H_N}(2) | \Phi \rangle \quad (34)$$

are the moments of CC equations corresponding to projections on the triply excited determinants missing in the final CI diagonalization space \mathcal{V}_{int} of a given CIPSI run, where the

similarity-transformed Hamiltonian

$$\overline{H}_N(2) = (H_N e^{T_1+T_2})_C = e^{-T_1-T_2} H_N e^{T_1+T_2} \quad (35)$$

is obtained using the singly and doubly excited clusters resulting from the ec-CC-II calculations. The $\ell_{ijk}^{abc}(2)$ coefficients, which are given by the expression

$$\ell_{ijk}^{abc}(2) = \langle \Phi | (\Lambda_1 + \Lambda_2) \overline{H}_N(2) | \Phi_{ijk}^{abc} \rangle / (\Delta E - \langle \Phi_{ijk}^{abc} | \overline{H}_N(2) | \Phi_{ijk}^{abc} \rangle), \quad (36)$$

are the deexcitation amplitudes that require solving the companion left CC equations for the one- and two-body components of the operator Λ that generates the CC bra state $\langle \Phi | (1 + \Lambda) e^{-T}$ (cf., e.g., ref 8), i.e.,

$$\langle \Phi | (1 + \Lambda_1 + \Lambda_2) [\overline{H}_N(2) - \Delta E \mathbf{1}] | \Phi_\alpha \rangle = 0, \quad (37)$$

where $|\Phi_\alpha\rangle$ represents the singly and doubly excited determinants.

As already alluded to in Section 2, the ec-CC approach, in which the ec-CC-II correlation energy ΔE , eq 7, is corrected for the missing T_3 effects not captured by the underlying CI calculations using correction δ_3 given by eq 33, defines the ec-CC-II₃ method. We use the above correction δ_3 rather than its simplified CCSD(T)-like analog adopted in the RMRCCSD(T) and ACI-CCSD(T) work,^{29,31} since it is well established that, in analogy to the completely renormalized CC approaches, such as CR-CC(2,3),^{80,81} the CC($P;Q$) moment corrections are a lot more robust.^{69,76,77} Furthermore, there are molecular applications where the CCSD(T)-type corrections, instead of improving the underlying results, make the results worse (see, e.g., ref 77 for a discussion). It should also be emphasized that the computational cost of determining the δ_3 correction to the ec-CC-II correlation energy is only twice the cost of calculating the corresponding (T) correction, i.e., the replacement of δ_3 , eq 33, by its (T) counterpart offers no significant computational benefits either.

At this time, our deterministic ec-CC-II and ec-CC-II₃ codes, along with the routines that allow one to perform the corresponding ec-CC-I calculations examined in Section 2.2, are capable of reading the non-CC wave functions for the subsequent cluster analysis and the CC computations based on eqs 5–7 and 33–37 from GAMESS (the determinantal ORMAS^{73,74} and FCI^{73–75} runs) and Quantum Package 2.0 (CIPSI calculations^{50,51}). We also have the semistochastic variant of the ec-CC codes that can work with the wave functions obtained with FCIQMC, as in the CAD-FCIQMC methodology introduced in ref 30 and further elaborated on in the Supporting Information to ref 35. The remaining information about our ec-CC codes used in this work can be found in Section 2.2.

We now move to the discussion of our CIPSI-based all-electron ec-CC-II and ec-CC-II₃ calculations for the C_{2v} -symmetric double bond dissociation of the water molecule, as described by the cc-pVDZ basis set, summarized in Tables 2 and 3. The information about the nuclear geometries used in these calculations has been provided in Section 2.2. In analogy to the ec-CC-I computations discussed in Section 2.2, we performed two sets of CIPSI-driven ec-CC-II and ec-CC-II₃ calculations. In the first set, summarized in Table 2, where we applied the CIPSI-based ec-CC-II and ec-CC-II₃ approaches to the equilibrium geometry, $R = R_e$, and two stretches of both O–H bonds, including $R = 2R_e$ and $3R_e$, we initiated each CIPSI run from the corresponding RHF wave function. In the second set, summarized in Table 3, where we focused on a single stretch of both O–H bonds, namely, $R = 2R_e$, we forced each CIPSI calculation preceding the ec-CC-II and ec-CC-II₃ steps to provide a complete treatment of the C_1 and C_2 operators by initiating the CIPSI runs from the wave function obtained with CISD. In each case, we considered multiple values of the input parameter $N_{\text{det}(\text{in})}$ used to terminate the CIPSI runs by sampling $N_{\text{det}(\text{in})}$ in a semi-logarithmic manner. In the case of the CIPSI calculations initiated from the single-determinantal RHF wave function (Table 2), the smallest value of $N_{\text{det}(\text{in})}$ was 1. As already mentioned in Section 2.2, the smallest value of $N_{\text{det}(\text{in})}$ used in the CIPSI calculations initiated from the CISD state had to be at least 3,416 (the number of $S_z = 0$ determinants defining the CISD ground-state

problem if the $A_1(C_{2v})$ symmetry is employed). The smallest value of $N_{\text{det(in)}}$ that we used in this case was 5,000.

The results in Tables 2 and 3 demonstrate that both ec-CC-II and ec-CC-II₃, especially the latter method, offer significant improvements over the underlying CIPSI computations. This is particularly true when the relatively small values of $N_{\text{det(in)}}$ and the similarly small CIPSI diagonalization spaces, as defined by $N_{\text{det(out)}}$, are employed. They also significantly improve the corresponding CCSD results, where T_3 and T_4 are assumed to be zero. As shown in Table 2, with as little as about 5,000–6,000 determinants in the CIPSI calculations initiated from RHF, which capture approximately 40–50 % of singles, 20–70 % of doubles, 1–2 % of triples, and 0.2 % of quadruples, the ec-CC-II approach reduces the approximately 8, 14, and 10 millihartree errors relative to FCI obtained with CIPSI at $R = R_e$, $2R_e$, and $3R_e$, respectively, to about 2–4 millihartree. The triples correction δ_3 , eq 33, used in the ec-CC-II₃ calculations, reduces these errors even further, to 0.012, 0.226, and 1.507 millihartree, respectively. These are impressive improvements, especially if we realize that the CISD and CCSD calculations, which use the same numbers of singly and doubly excited amplitudes as ec-CC-II and only slightly smaller numbers of excitation amplitudes than the $N_{\text{det(in)}} = 5,000$ CIPSI runs, produce much larger errors, which are more than 12 millihartree at $R = R_e$, more than 72 millihartree at $R = 2R_e$, and almost 165 millihartree at $R = 3R_e$ in the case of CISD and about 4, 22, and 11 millihartree, respectively, when the CCSD approach is employed (cf. Table 1). As a matter of fact, by comparing the results in Tables 1 and 2, we can see that the $N_{\text{det(in)}} = 5,000$ ec-CC-II₃ calculations initiated from RHF are considerably more accurate than the CCSDT, CISDTQ, and even CISDTQP calculations, which are more expensive by orders of magnitude and which use 90,279, 1,291,577, and 10,502,233 $S_z = 0$ excitation amplitudes, when the $A_1(C_{2v})$ symmetry is employed, as opposed to 3,145 amplitudes used by the underlying ec-CC-II approach and about 5,000–6,000 determinants included in the CIPSI diagonalizations needed to extract the T_3 and T_4 clusters for the ec-CC computations. Interestingly, while the CIPSI-driven ec-CC-II₃ method using $N_{\text{det(in)}} = 5,000$ is less accurate

than the CCSDTQ approach in the $R = R_e-2R_e$ region, it becomes competitive with it when the largest stretch of both O–H bonds in water considered in this study, i.e., $R = 3R_e$, is examined, reducing the -4.733 millihartree error relative to FCI obtained with CCSDTQ by more than a factor of 3. Compared to ec-CC-II, there is an extra cost associated with the determination of the triples correction δ_3 in the ec-CC-II₃ calculations, but the computational costs associated with this noniterative correction, being similar to those of CCSD(T), are less than the cost of a single iteration of CISDT or CCSDT. One also has to keep in mind that, in analogy to CCSD(T), one does not have to store higher-than-two-body quantities when forming the triples correction defined by eqs 33–37.

The results of the ec-CC-II and ec-CC-II₃ calculations employing the T_3 and T_4 amplitudes extracted from the CIPSI wave functions become even more accurate when the CIPSI diagonalization spaces start growing. For example, when the wave function termination parameter $N_{\text{det(in)}}$ is set at 50,000, which translates into about 80,000–90,000 determinants participating in the final Hamiltonian diagonalizations of the corresponding CIPSI runs, the ec-CC-II calculations reduce the 2.612, 2.436, and 0.906 millihartree errors relative to FCI at $R = R_e$, $2R_e$, and $3R_e$, respectively, obtained with CIPSI, by factors of 3–4, to 0.626 millihartree at $R = R_e$, 0.788 millihartree at $R = 2R_e$, and 0.341 millihartree at $R = 3R_e$. The δ_3 correction reduces the already small errors obtained with the CIPSI-driven ec-CC-II approach at $R = R_e$ and $2R_e$ even further, to 0.168 and 0.515 millihartree, respectively. The ec-CC-II₃ calculations do not improve the underlying ec-CC-II result at $R = 3R_e$ any longer, most likely because the δ_3 correction defined by eq 33 takes care of only the missing T_3 correlations not captured by CIPSI, without correcting the ec-CC-II energies for the missing T_4 effects, which at $R = 3R_e$ may become substantial (cf., e.g., the large difference between the CCSDTQ and CCSDT energies in Table 1). On the other hand, the 0.358 millihartree error obtained with ec-CC-II₃ in a highly challenging multi-reference situation created by the $R = 3R_e$ structure of the water molecule is a very accurate result. One has to keep in mind that the much more expensive CISDTQ and CCSDTQ methods, which

use 1,291,577 excitation amplitudes, as opposed to $N_{\text{det}(\text{out})} = 92,707$ determinants in the last CIPSI diagonalization space corresponding to $N_{\text{det}(\text{in})} = 50,000$ and 3,145 singles and doubles participating in the ec-CC steps, combined with the relatively inexpensive noniterative correction δ_3 , produce the 16.150 and -4.733 millihartree errors, respectively, when the $R = 3R_e$ geometry is considered. As in the previously discussed $N_{\text{det}(\text{in})} = 5,000$ case, the $N_{\text{det}(\text{in})} = 50,000$ CIPSI-based ec-CC-II₃ calculations are also more accurate than CISDTQP, which uses 10,502,233 excitation amplitudes.

When we look at the overall picture emerging from the results reported in Tables 2 and 3, it is quite clear that the CIPSI-driven ec-CC-II and ec-CC-II₃ computations, especially the latter ones, offer a rapid convergence toward FCI with the relatively small CIPSI diagonalization spaces. As shown, for example, in Tables 2 and 3, when one uses about 1,000,000 determinants in the final diagonalizations of the CIPSI runs, both the uncorrected ec-CC-II and the corrected ec-CC-II₃ calculations recover the FCI energetics at all three geometries of the water molecule examined in this work, including the most challenging $R = 3R_e$ structure, to within 0.1 millihartree. To appreciate this result, one has to keep in mind that 1,000,000 determinants in the diagonalization space is nowhere near the dimension of the FCI ground-state problem, which is 451,681,246 if the $S_z = 0$ $A_1(C_{2v})$ -symmetric determinants are considered. What certainly helps the ec-CC-II and ec-CC-II₃ calculations in achieving this remarkable performance is the aforementioned tempered growth of the wave function in the consecutive CIPSI iterations, which allows the CIPSI algorithm, as implemented in the Quantum Package 2.0 software utilized in this study, to efficiently sample the many-electron Hilbert space, without saturating the lower-rank excitation manifolds, especially the excitations through quadruples, too early. As already demonstrated in Section 2, mathematically and numerically, if CIPSI saturated the lower-rank excitation manifolds too rapidly, without bringing information about higher-than-quadruply excited contributions, our ec-CC-II computations would collapse onto the results of the respective Hamiltonian diagonalizations. This emphasizes the significance of the appropriate design of the CI (in

general, non-CC) methodologies used to provide information about the T_3 and T_4 clusters in ec-CC considerations. Our computations suggest that the current design of the CIPSI algorithm in Quantum Package 2.0 is well suited for the ec-CC-II and ec-CC-II₃ approaches developed in this study.

Having stated all of the above, one cannot ignore the fact that the CIPSI approach can be very efficient in its own right, especially when the variational energies E_{var} resulting from the underlying CI diagonalizations are corrected for the remaining correlation effects with the help of the aforementioned and easy-to-determine second-order multi-reference MBPT corrections $\Delta E^{(2)}$. As shown, for example, in Table 2, when the final diagonalizations of the CIPSI runs involve about 1,000,000 determinants, the $E_{\text{var}} + \Delta E^{(2)}$ energies are within a few microhartree from FCI, independent of the nuclear geometry, despite the fact that the FCI space is about 500 times larger. When $N_{\text{det(in)}} = 1,000,000$, which translates into diagonalization spaces on the order of 1.2–1.4 million, the $E_{\text{var}} + \Delta E^{(2)}$ energies reported in Table 2 are competitive with their ec-CC-II and ec-CC-II₃ counterparts. Even with as little as about 80,000–90,000 determinants in the final diagonalizations of the CIPSI runs, which result from setting the $N_{\text{det(in)}}$ parameter at 50,000, the $E_{\text{var}} + \Delta E^{(2)}$ energies are still within 0.1 millihartree from FCI. While the perturbatively corrected CIPSI calculations for larger many-electron systems and larger basis sets may require additional extrapolations to achieve similarly accurate results,^{51,62} the fact of the matter remains that CIPSI represents a powerful computational tool capable of generating high-quality results by itself. The CIPSI-driven ec-CC-II and ec-CC-II₃ approaches are capable of substantially improving the purely variational CIPSI energies and the results of lower-rank CC calculations, but one has to keep in mind that CIPSI and other modern variants of selected CI techniques can be made very accurate too, i.e., the benefits offered by the ec-CC framework utilizing such techniques may not always be as great as desired.

4 CONCLUSIONS

One of the most interesting ways of extending the applicability of single-reference CC approaches to multi-reference and strongly correlated systems is offered by the ec-CC formalism. The key idea of all ec-CC methods is to solve the CC equations for the lower-rank cluster components, such as T_1 and T_2 , in the presence of their higher-order T_n counterparts (typically, T_3 and T_4) extracted from a non-CC source that behaves well in situations characterized by stronger nondynamic correlations. In this paper, we have focused on the ec-CC methods, in which one solves the CC equations projected on the singly and doubly excited determinants, eqs 5 and 6, respectively, for the T_1 and T_2 clusters using the T_3 and T_4 contributions obtained via cluster analysis of truncated CI wave functions.

The present study has had two main objectives. The first objective has been a thorough examination of the mathematical content of the ec-CC equations, backed by the appropriate numerical analysis, in which we have attempted to identify the truncated CI states that, after extracting the T_n components of the cluster operator T with $n = 1-4$ from them via the cluster analysis procedure adopted in all ec-CC considerations, satisfy eqs 5 and 6. This is an important topic, since, by solving eqs 5 and 6 for the T_1 and T_2 clusters in the presence of the T_3 and T_4 amplitudes extracted from such states, the ec-CC procedure can only return back the corresponding CI energies, without improving them at all. The second objective has been the exploration of a novel flavor of the ec-CC approach in which the wave functions used to generate the required T_3 and T_4 contributions are obtained by the cluster analysis of the truncated CI wave functions resulting from one of the most successful selected CI methods abbreviated as CIPSI.

We have demonstrated that the ec-CC calculations performed by solving eqs 5 and 6, where the T_3 and T_4 components are obtained by cluster analysis of the CI wave functions that describe singles and doubles fully and higher-than-double excitations in a complete or partial manner and where all T_3 and T_4 amplitudes generated in this way are kept, as in the ec-CC-I protocol discussed in Section 2, return back the underlying CI energies. This means that

the ec-CC computations, which use the wave functions obtained with the conventional CI truncations, such as CISD, CISDT, CISDTQ, etc., or with any other CI method that provides a complete treatment of the single and double excitation manifolds, offer no improvements over CI if no *a posteriori* modifications are made in T_3 and T_4 extracted from CI. In reality, i.e., in typical applications of the CI-based ec-CC methodology, one disregards the purely disconnected T_3 and T_4 amplitudes of the type of eqs 12 and 13, for which the corresponding CI excitation coefficients are zero, as in the ec-CC-II algorithm discussed in Sections 2 and 3, but this does not prevent the collapse of the resulting ec-CC energies onto their CI counterparts. As shown in this work, mathematically and through numerical examples, the ec-CC-II approach may offer improvements over the underlying CI calculations, but only if the triply and quadruply excited manifolds considered in CI are incomplete. Once the CI calculation captures all triples and quadruples, as in CISDTQ, CISDTQP, CISDTQPH, etc., or in any other CI truncation that treats singles through quadruples fully, the ec-CC-I and ec-CC-II schemes examined in our study become equivalent and the ec-CC computations offer no benefits compared to CI, while adding to the computational cost. In other words, in order for the ec-CC computations based on eqs 5 and 6 to significantly improve the energetics obtained with the underlying CI approach, it is essential to avoid a complete or nearly complete treatment of the triple and quadruple excitation manifolds. In that case, after solving eqs 5 and 6 for T_1 and T_2 in the presence of T_3 and T_4 extracted from CI, in which the amplitudes that do not have the companion triple and quadruple excitation CI coefficients are ignored, it is useful to correct the resulting ec-CC-II energies for the remaining T_3 and T_4 or at least T_3 correlations, as in the RMRCCSD(T) approach of ref 29 or the CIPSI-driven ec-CC-II₃ method introduced in this work, to name representative examples. We have also considered higher-order ec-CC-I and ec-CC-II variants that solve for higher-than-two-body components of the cluster operator T and examined their relations with the underlying CI approaches.

Our mathematical and numerical analyses imply that the truncated CI wave functions

that are best suited for the ec-CC computations are those that attempt to efficiently sample the many-electron Hilbert space without saturating the lower-rank excitation manifolds, especially the excitations through quadruples, too rapidly. As shown in this work, the modern formulation of the CIPSI approach, developed in refs 50,51, which achieves a tempered growth of the wave function through a systematic sequence of CI calculations, combined with perturbative and stochastic analyses of the excitation spaces used in Hamiltonian diagonalizations, is capable of providing such CI states. By examining the C_{2v} -symmetric double bond dissociation of the water molecule, including the very challenging region where both O–H bonds are stretched by a factor of 3, so that even the sophisticated levels of the CC theory, such as full CCSDT and CCSDTQ, struggle, we have demonstrated that the CIPSI-based ec-CC-II method, described in Section 3, is capable of providing highly accurate results with the relatively low computational costs, especially when the ec-CC-II energies are corrected for the missing T_3 correlations via the ec-CC-II₃ scheme. The CIPSI-driven ec-CC-II₃ energies are so accurate that they are competitive with those obtained with the much more expensive high-level CC and CI methods, such as CCSDTQ, CISDTQP, or even CISDTQPH. Most remarkably, the ec-CC-II and ec-CC-II₃ computations, especially the latter ones, offer a rapid convergence toward FCI, reaching submillihartree accuracies with the relatively small CIPSI diagonalization spaces used to determine T_3 and T_4 . The fast convergence of the energies obtained in the CIPSI-enabled ec-CC-II runs toward FCI is reminiscent of the FCIQMC-enabled ec-CC computations using the CAD-FCIQMC method, observed in refs 30,35. This only reinforces our view that the CI approaches which are capable of efficiently sampling the many-electron Hilbert space through a tempered evolution of the wave function, without populating the lower-rank excitation manifolds, especially the excitations through quadruples, too fast, benefit the ec-CC computations most.

While our initial tests of the CIPSI-driven ec-CC-II and ec-CC-II₃ approaches reported in this study are very promising, encouraging us to continue our work in this direction, the present study has also pointed out that the underlying CIPSI method, especially when

one adds the second-order multi-reference MBPT corrections to the variational energies obtained in the CIPSI Hamiltonian diagonalizations, can be made very accurate as well, being competitive with the ec-CC-II₃ results. This is not a criticism of the idea of ec-CC, but, rather, a recognition of the fact that the new generations of selected CI techniques, such as those developed in refs 47,48,50,51,55–61, and the stochastic CI approaches, such as FCIQMC,^{37–40} have become highly competitive with the best CC solutions (cf., e.g., refs 35,62 for selected recent examples).

It would be important to investigate if our initial observations regarding the performance of the CIPSI-based ec-CC-II and ec-CC-II₃ approaches reported in this study remain true in a wider range of molecular applications. Furthermore, it would be interesting to examine if the ec-CC approaches based on other selected CI methods developed by various groups in recent years, especially the semi-stochastic CI approaches enabling a highly efficient sampling of the many-electron Hilbert space, such as the heat-bath CI framework of refs 59–61, are as accurate and as efficient as the CIPSI-enabled ec-CC-II and ec-CC-II₃ schemes examined here. It would also be important to investigate if our ec-CC-II₃ results could further be improved by correcting the CIPSI-driven ec-CC-II energies for the missing T_3 as well as T_4 correlation effects not captured during CIPSI runs, rather than the missing T_3 correlations only. In analogy to the triples correction δ_3 adopted in this work, we could take advantage of the formulas that we previously used to develop and benchmark the $CC(P;Q)$ approaches correcting the active-space CC energies, such as CCSDtq, for the missing triples and quadruples.^{69,76,82,83} Such corrections might also benefit the aforementioned semi-stochastic CAD-FCIQMC methodology based in the cluster analysis of FCIQMC wave functions, which we have been pursuing in parallel with the ec-CC development work reported in this article.

Acknowledgement

This work has been supported by the Chemical Sciences, Geosciences and Biosciences Divi-

sion, Office of Basic Energy Sciences, Office of Science, U.S. Department of Energy (Grant No. DE-FG02-01ER15228 to P.P) and Phase I and II Software Fellowships awarded to J.E.D. by the Molecular Sciences Software Institute funded by the National Science Foundation grant ACI-1547580.

APPENDIX A: PROOF OF THE EQUIVALENCE OF EQ 17, WITH THE CORRELATION ENERGY DEFINED BY EQ 19, AND EQS 5–7 BASED ON EQS 20, 24, AND 25

The main purpose of this appendix is to demonstrate that the subsystem of CI equations for the ground-state wave function $|\Psi\rangle$ defined by eqs 14–16, corresponding to the projections on the singly and doubly excited determinants, as in eq 17, where the correlation energy $\Delta E^{(CI)}$ is calculated using eq 19, can be transformed into the CC amplitude equations projected on singles and doubles, represented by eqs 3 and 4 or 5 and 6, with the CC energy given by eq 7, if the cluster operator T is defined by eq 20. We begin by rewriting eq 17 with the help of eq 20, which allows us to convert the CI expansion for $|\Psi\rangle$, eq 14, to a CC-type expression, eq 1, while taking advantage of the property of the exponential ansatz given by eq 24. We obtain,

$$\langle\Phi_\alpha|e^T(H_N e^T)_C|\Phi\rangle = \Delta E^{(CI)} \langle\Phi_\alpha|e^T|\Phi\rangle, \quad (\text{A.1})$$

where the CI correlation energy $\Delta E^{(CI)}$, eq 19, becomes

$$\Delta E^{(CI)} = \langle\Phi|H_N e^T|\Phi\rangle = \langle\Phi|(H_N e^T)_{FC}|\Phi\rangle, \quad (\text{A.2})$$

in agreement with the CC energy formula given by eq 7. Let us recall that the $|\Phi_\alpha\rangle$ states entering eq A.1 are the determinants that span subspace $\mathcal{H}^{(PA)}$ matching the $C^{(PA)}|\Phi\rangle$

component of $|\Psi\rangle$ which, in this particular analysis, are a short-hand notation for the singly and doubly excited determinants, $|\Phi_i^a\rangle$ and $|\Phi_{ij}^{ab}\rangle$, respectively.

The next step is the insertion of the resolution of the identity in the many-electron Hilbert space \mathcal{H} , eq 25, between e^T and $(H_N e^T)_C$ on the left-hand side of eq A.1. This allows us to rewrite eq A.1 as follows:

$$\Lambda_\alpha^{(1)} + \Lambda_\alpha^{(2)} + \Lambda_\alpha^{(3)} + \Lambda_\alpha^{(4)} = \Delta E^{(\text{CI})} \langle \Phi_\alpha | e^T | \Phi \rangle, \quad (\text{A.3})$$

where

$$\Lambda_\alpha^{(1)} = \langle \Phi_\alpha | e^T | \Phi \rangle \langle \Phi | (H_N e^T)_{FC} | \Phi \rangle \equiv \Delta E^{(\text{CI})} \langle \Phi_\alpha | e^T | \Phi \rangle, \quad (\text{A.4})$$

$$\Lambda_\alpha^{(2)} = \sum_{\alpha'} \langle \Phi_\alpha | e^T | \Phi_{\alpha'} \rangle \langle \Phi_{\alpha'} | (H_N e^T)_C | \Phi \rangle, \quad (\text{A.5})$$

$$\Lambda_\alpha^{(3)} = \sum_{\beta} \langle \Phi_\alpha | e^T | \Phi_\beta \rangle \langle \Phi_\beta | (H_N e^T)_C | \Phi \rangle, \quad (\text{A.6})$$

and

$$\Lambda_\alpha^{(4)} = \sum_{\gamma} \langle \Phi_\alpha | e^T | \Phi_\gamma \rangle \langle \Phi_\gamma | (H_N e^T)_C | \Phi \rangle, \quad (\text{A.7})$$

with $|\Phi_\alpha\rangle, |\Phi_{\alpha'}\rangle \in \mathcal{H}^{(P_A)}$, $|\Phi_\beta\rangle \in \mathcal{H}^{(P_B)}$, and $|\Phi_\gamma\rangle \in \mathcal{H}^{(Q)}$. We recall that $\mathcal{H}^{(P_B)}$ is a subspace spanned by the determinants $|\Phi_\beta\rangle$ that match the content of the $C^{(P_B)}$ operator, eq 16, and $\mathcal{H}^{(Q)} = (\mathcal{H}^{(P)} \oplus \mathcal{H}^{(P_A)} \oplus \mathcal{H}^{(P_B)})^\perp$, with $\mathcal{H}^{(P)}$ spanned by the reference determinant $|\Phi\rangle$, is a subspace spanned by the remaining determinants, designated as $|\Phi_\gamma\rangle$, which are not included in the CI wave function $|\Psi\rangle$ defined by eqs 14–16. In writing eq A.4, we took advantage of the energy formula given by eq A.2.

Let us analyze each contribution $\Lambda_\alpha^{(k)}$, $k = 1-4$, to eq A.3. Since we have made the assumption that the $|\Phi_\alpha\rangle$ states represent the singly and doubly excited determinants and $|\Phi_\beta\rangle$ and $|\Phi_\gamma\rangle$ are at least the triples, the $\langle \Phi_\alpha | e^T | \Phi_\beta \rangle$ and $\langle \Phi_\alpha | e^T | \Phi_\gamma \rangle$ matrix elements in eqs A.6 and A.7 vanish, i.e., $\Lambda_\alpha^{(3)} = \Lambda_\alpha^{(4)} = 0$. At the same time, $\Lambda_\alpha^{(1)}$, eq A.4, cancels out the

right hand side of eq A.3. This means that eq A.3 reduces to

$$\Lambda_\alpha^{(2)} = 0, \quad (\text{A.8})$$

with $\Lambda_\alpha^{(2)}$ defined by eq A.5. Since in the specific case considered here $|\Phi_\alpha\rangle$ and $|\Phi_{\alpha'}\rangle$ are the singly and doubly excited determinants, the definition of the cluster operator T , eq 20, implies that $e^T = 1 + C^{(PA)} + C^{(PB)}$, and the C_2 and $C^{(PB)}$ operators generate at least double excitations, we can rewrite the $\langle\Phi_\alpha|e^T|\Phi_{\alpha'}\rangle$ term seen in eq A.5 in the following manner:

$$\langle\Phi_\alpha|e^T|\Phi_{\alpha'}\rangle \equiv \langle\Phi_\alpha|(1 + C_1 + C_2 + C^{(PB)})|\Phi_{\alpha'}\rangle = \delta_{\alpha\alpha'} + \langle\Phi_\alpha|C_1|\Phi_{\alpha'}\rangle, \quad (\text{A.9})$$

where $\delta_{\alpha\alpha'}$ is the usual Kronecker delta. By substituting eq A.9 into eq A.5 and using eq A.8, we immediately obtain

$$\Lambda_\alpha^{(2)} = \langle\Phi_\alpha|(H_N e^T)_C|\Phi\rangle + \sum_{\alpha'} \langle\Phi_\alpha|C_1|\Phi_{\alpha'}\rangle \langle\Phi_{\alpha'}|(H_N e^T)_C|\Phi\rangle = 0. \quad (\text{A.10})$$

We now examine the system of equations represented by eq A.10. Let us start with the case in which $|\Phi_\alpha\rangle = |\Phi_i^a\rangle$. Since C_1 generates single excitations and $|\Phi_{\alpha'}\rangle$'s in eq A.10 are at least the singly excited determinants, $\langle\Phi_\alpha|C_1|\Phi_{\alpha'}\rangle = 0$. We can, therefore, conclude that the CI equations projected on the singly excited determinants, eq 17 with $|\Phi_\alpha\rangle = |\Phi_i^a\rangle$ or eq 21, which are equivalent to eq A.10 in which $|\Phi_\alpha\rangle = |\Phi_i^a\rangle$, reduce to the CC equations projected on singles given by eq 3 or, more explicitly, eq 5.

In the case of the projections on the doubly excited determinants $|\Phi_{ij}^{ab}\rangle$, i.e., when $|\Phi_\alpha\rangle = |\Phi_{ij}^{ab}\rangle$, we can give eq A.10 the following form:

$$\langle\Phi_{ij}^{ab}|(H_N e^T)_C|\Phi\rangle + \sum_{k,c} \langle\Phi_{ij}^{ab}|C_1|\Phi_k^c\rangle \langle\Phi_k^c|(H_N e^T)_C|\Phi\rangle = 0, \quad (\text{A.11})$$

where we utilized the fact that the $\langle\Phi_{ij}^{ab}|C_1|\Phi_{\alpha'}\rangle$ matrix element vanishes unless $|\Phi_{\alpha'}\rangle$ is a

singly excited determinant. Since we have already demonstrated that the cluster operator T , eq 20, satisfies eq 3, i.e., $\langle \Phi_k^c | (H_N e^T)_C | \Phi \rangle = 0$, eq A.11 simplifies to eq 4. This means that the CI equations projected on the doubly excited determinants, eq 17 with $|\Phi_\alpha\rangle = |\Phi_{ij}^{ab}\rangle$ or eq 22, which are equivalent to eq A.10 in which $|\Phi_\alpha\rangle = |\Phi_{ij}^{ab}\rangle$, reduce to the CC equations projected on doubles given by eq 4 or, more explicitly, eq 6. This concludes our first proof of the equivalence of the CI eqs 17 and 19 and their CC counterparts represented by eqs 3, 4, and 7 or 5–7.

As mentioned at the end of Section 2.1, one can extend the above considerations to higher-order ec-CC variants, in which the excitation operators $C^{(P_A)}$ and $C^{(P_B)}$ that enter the CI wave function $|\Psi\rangle$ through eq 14 are defined by eqs 30 and 31. In this case, subspace $\mathcal{H}^{(P_A)}$, which matches the content of $C^{(P_A)}$, is spanned by all determinants $|\Phi_\alpha\rangle$ with the excitation ranks ranging from 1 to m_A , where $m_A \geq 2$, and determinants $|\Phi_\beta\rangle \in \mathcal{H}^{(P_B)}$ that match the many-body components $C_n^{(P_B)}$ of operator $C^{(P_B)}$, assuming that $C^{(P_B)} \neq 0$, have the excitation ranks exceeding m_A . In order to prove the equivalence of eq 17, with the correlation energy defined by 19, and the CC system defined by eq 32 in this generalized case, we follow the same procedure as described above, adjusting it to the contents of operators $C^{(P_A)}$ and $C^{(P_B)}$ and subspaces $\mathcal{H}^{(P_A)}$ and $\mathcal{H}^{(P_B)}$. It is immediately obvious that eqs A.1–A.8 still hold. In particular, $\Lambda_\alpha^{(1)}$ cancels out the right hand side of eq A.3 and matrix elements $\langle \Phi_\alpha | e^T | \Phi_\beta \rangle$ and $\langle \Phi_\alpha | e^T | \Phi_\gamma \rangle$ that enter the $\Lambda_\alpha^{(3)}$ and $\Lambda_\alpha^{(4)}$ contributions to eq A.3 vanish, since the many-body ranks of determinants $|\Phi_\alpha\rangle \in \mathcal{H}^{(P_A)}$ do not exceed m_A , the excitation levels of $|\Phi_\beta\rangle$ and $|\Phi_\gamma\rangle$, which belong to $\mathcal{H}^{(P_B)}$ and $\mathcal{H}^{(Q)}$, respectively, are at least $m_A + 1$, and $e^T = 1 + C^{(P_A)} + C^{(P_B)}$. With the generalized definitions of the excitation operators $C^{(P_A)}$ and $C^{(P_B)}$ considered here, eq A.8 can be given the following form:

$$\Lambda_\alpha^{(2)} = \langle \Phi_\alpha | (H_N e^T)_C | \Phi \rangle + \sum_{\alpha'} \langle \Phi_\alpha | \tilde{C} | \Phi_{\alpha'} \rangle \langle \Phi_{\alpha'} | (H_N e^T)_C | \Phi \rangle = 0, \quad (\text{A.12})$$

where

$$\tilde{C} = \sum_{n=1}^{m_A-1} C_n, \quad (\text{A.13})$$

since the excitation ranks of determinants $|\Phi_\alpha\rangle$ and $|\Phi_{\alpha'}\rangle$ belonging to $\mathcal{H}^{(P_A)}$ range from 1 to m_A and operator $C^{(P_B)}$ generates higher-than- m_A -fold excitations, so that

$$\langle \Phi_\alpha | e^T | \Phi_{\alpha'} \rangle \equiv \langle \Phi_\alpha | (1 + \sum_{n=1}^{m_A} C_n + C^{(P_B)}) | \Phi_{\alpha'} \rangle = \delta_{\alpha\alpha'} + \langle \Phi_\alpha | \tilde{C} | \Phi_{\alpha'} \rangle, \quad (\text{A.14})$$

with \tilde{C} defined by eq A.13.

As in the previously considered $m_A = 2$ case, we examine the system represented by eq A.12, which we can do in a recursive manner starting from $|\Phi_\alpha\rangle = |\Phi_i^a\rangle$. When $|\Phi_\alpha\rangle = |\Phi_i^a\rangle$, matrix element $\langle \Phi_\alpha | \tilde{C} | \Phi_{\alpha'} \rangle$ vanishes, since $|\Phi_{\alpha'}\rangle$ is at least a singly excited determinant and \tilde{C} defined by eq A.13 generates at least single excitations. This immediately leads to the CC equations projected on the singly excited determinants, eq 3, i.e., eq 32 is satisfied when $|\Phi_\alpha\rangle = |\Phi_i^a\rangle$. Moving on, when $|\Phi_\alpha\rangle = |\Phi_{ij}^{ab}\rangle$, $\langle \Phi_\alpha | \tilde{C} | \Phi_{\alpha'} \rangle = 0$ unless $|\Phi_{\alpha'}\rangle$ is a singly excited determinant, but since the CC equations projected on singles are already satisfied, the summation over α' in eq A.12 vanishes and eq A.12 reduces to the CC equations projected on doubles, eq 4, which means that eq 32 remains true for $|\Phi_\alpha\rangle = |\Phi_{ij}^{ab}\rangle$. Continuing (assuming that $m_A > 2$), when $|\Phi_\alpha\rangle = |\Phi_{ijk}^{abc}\rangle$, $\langle \Phi_\alpha | \tilde{C} | \Phi_{\alpha'} \rangle$ is zero unless $|\Phi_{\alpha'}\rangle$ is a singly or doubly excited determinant. Again, since the CC equations projected on singles and doubles are already satisfied, the summation over α' in eq A.12 becomes zero and we obtain $\langle \Phi_{ijk}^{abc} | (H_N e^T)_C | \Phi \rangle = 0$, i.e., eq 32 is satisfied in the $|\Phi_\alpha\rangle = |\Phi_{ijk}^{abc}\rangle$ case. One can repeat the same procedure for the projections on higher-rank determinants $|\Phi_\alpha\rangle$ in eq A.12 that belong to subspace $\mathcal{H}^{(P_A)}$. In the final stage of this recursive analysis, i.e., when $|\Phi_\alpha\rangle$ is an m_A -tuply excited determinant, eq 32 remains true as well, since $\langle \Phi_\alpha | \tilde{C} | \Phi_{\alpha'} \rangle$ vanishes unless the excitation rank of $|\Phi_{\alpha'}\rangle$ is at most $m_A - 1$ and the CC equations projected on up to $(m_A - 1)$ -tuply excited determinants are already satisfied. This means that $\langle \Phi_\alpha | (H_N e^T)_C | \Phi \rangle$ is zero, i.e., eq 32 holds once again. In other words, eq 32 remains true for all determinants

$|\Phi_\alpha\rangle \in \mathcal{H}^{(P_A)}$, i.e., eq 17, with the correlation energy defined by 19, is equivalent to the CC system defined by eq 32 when the excitation operators $C^{(P_A)}$ and $C^{(P_B)}$ that enter the CI wave function $|\Psi\rangle$ through eq 14 are defined by eqs 30 and 31 and subspace $\mathcal{H}^{(P_A)}$, which matches the content of $C^{(P_A)}$, is spanned by all determinants $|\Phi_\alpha\rangle$ with the excitation ranks ranging from 1 to m_A .

APPENDIX B: DIAGRAMMATIC PROOF OF THE EQUIVALENCE OF EQ 17, WITH THE CORRELATION ENERGY DEFINED BY EQ 19, OR EQS 21–23 AND EQS 5–7

In this appendix, we provide an alternative proof of the equivalence of eqs 5–7 and 21–23 using a diagrammatic approach. As in the case of the algebraic derivation presented in Appendix A, the only assumption that we make regarding the CI state $|\Psi\rangle$ used to provide information about the T_3 and T_4 clusters for ec-CC considerations is the full treatment of the C_1 and C_2 components. This means that all of the mathematical manipulations in this appendix apply to conventional as well as unconventional truncations in the CI excitation operator, as defined by eqs 14–16, in addition to FCI. The diagrammatic derivation of the equivalence of eqs 5–7 and 21–23 is accomplished by starting from the CC equations corresponding to projections on singles and doubles, eqs 5 and 6, respectively, and, after performing cluster analysis of the CI wave function $|\Psi\rangle$ with the help of eq 11, converting them to the analogous eqs 21 and 22, with the correlation energy defined by eq 23, which are part of the CI eigenvalue problem for $|\Psi\rangle$ used to determine the three- and four-body clusters. To facilitate our presentation, throughout this appendix we drop the ‘ (P_B) ’ superscript in the $C_n^{(P_B)}$ components of operator $C^{(P_B)}$, eq 16, associated with higher-than-doubly excited contributions to $|\Psi\rangle$.

The first step is to express eqs 5 and 6 in terms of the C_1 – C_4 operators by using the

relationships between the T_n and C_n components given by eq 11. In the case of the singles projections, the correspondence between the various $(H_N e^T)_C$ terms appearing in eq 5 and their counterparts resulting from the application of eq 11 is provided in Chart B.1. As shown in Chart B.1, all contributions containing products of C_n components other than the unlinked terms, marked in red, in which the fully connected operator products $(F_N C_1)_{FC}$ and $(V_N C_2)_{FC}$ that contribute to the correlation energy multiply C_1 , cancel out. As a result, the CC equations corresponding to projections on the singly excited determinants, eq 5, become

$$\langle \Phi_i^a | [F_N + (F_N C_1)_C + (F_N C_2)_C + (V_N C_1)_C + (V_N C_2)_C + (V_N C_3)_C + \Theta_1] | \Phi \rangle = 0, \quad (\text{B.1})$$

where

$$\Theta_1 = -[(F_N C_1)_{FC} C_1 + (V_N C_2)_{FC} C_1] \quad (\text{B.2})$$

represents the terms highlighted in Chart B.1 in red. Focusing on the Θ_1 contribution to eq B.1, we obtain

$$\begin{aligned} \langle \Phi_i^a | \Theta_1 | \Phi \rangle &= -\langle \Phi_i^a | [(F_N C_1)_{FC} C_1 + (V_N C_2)_{FC} C_1] | \Phi \rangle \\ &= -\langle \Phi_i^a | [(F_N C_1)_{FC} + (V_N C_2)_{FC}] C_1 | \Phi \rangle \\ &= -\Delta E^{(\text{CI})} \langle \Phi_i^a | C_1 | \Phi \rangle, \end{aligned} \quad (\text{B.3})$$

where we used eq 23 for the CI correlation energy $\Delta E^{(\text{CI})}$, which, after replacing H_N by the sum of F_N and V_N , is equivalent to

$$\Delta E^{(\text{CI})} = \langle \Phi | [(F_N C_1)_{FC} + (V_N C_2)_{FC}] | \Phi \rangle. \quad (\text{B.4})$$

Inserting eq B.3 for $\langle \Phi_i^a | \Theta_1 | \Phi \rangle$ back to eq B.1 and moving the energy-dependent term

$\Delta E^{(\text{CI})} \langle \Phi_i^a | C_1 | \Phi \rangle$ to the right-hand side of the resulting expression, we arrive at

$$\langle \Phi_i^a | [F_N + (F_N C_1)_C + (F_N C_2)_C + (V_N C_1)_C + (V_N C_2)_C + (V_N C_3)_C] | \Phi \rangle = \Delta E^{(\text{CI})} \langle \Phi_i^a | C_1 | \Phi \rangle, \quad (\text{B.5})$$

which is equivalent to eq 21, when expressed in terms of the one- and two-body components of H_N . This completes the proof of the equivalence of eqs 5 and 21.

A similar analysis can be performed for the CC equations corresponding to projections on the doubly excited determinants, eq 6. The correspondence between the various $(H_N e^T)_C$ terms contributing to eq 6 and their counterparts obtained by using eq 11 is shown in Chart B.2. In this case, despite the cancellation of the majority of the nonlinear terms in the C_n components resulting from the application of eq 11, the emergence of the CI equations projected on doubles, eq 22, from eq 6 is not as obvious as in the previously examined singles projections. As shown in Chart B.2, in addition to the unlinked terms, marked in red and green, in which the fully connected operator products $(F_N C_1)_{FC}$ and $(V_N C_2)_{FC}$ that contribute to the correlation energy multiply C_2 and $\frac{1}{2}C_1^2$, we see the appearance of the disconnected quantities, marked in blue, where the $(F_N C_1)_C$, $(F_N C_2)_C$, $(V_N C_1)_C$, $(V_N C_2)_C$, and $(V_N C_3)_C$ connected operator products multiply C_1 . The Hugenholtz diagrams emerging from the $V_N C_1 C_3$ and $\frac{1}{2}V_N C_2^2$ operator products, which result from the application of eq 11 to the $\langle \Phi_{ij}^{ab} | (V_N T_4)_C | \Phi \rangle$ contribution to eq 6 and which correspond to the second through fifth expressions contributing to $(V_N T_4)_C$ in Chart B.2, are shown in Figure B.1. It should be noted that the T_4 component (emphasized in Figure B.1 by a dashed oval) resulting from the cluster analysis defined by eq 11 is a strictly connected quantity (in an MBPT sense) only in a FCI limit.

After removing the nonlinear terms in C_n components that cancel out and grouping the remaining contributions to the CC equations corresponding to projections on the doubly

excited determinants according to their color in Chart B.2, eq 6 becomes

$$\begin{aligned} \langle \Phi_{ij}^{ab} | [(F_N C_2)_C + (F_N C_3)_C + V_N + (V_N C_1)_C + (V_N C_2)_C + (V_N C_3)_C + (V_N C_4)_C \\ + \Theta' + \Theta'' + \Theta_2] | \Phi \rangle = 0, \end{aligned} \quad (\text{B.6})$$

where

$$\Theta' = -[(F_N C_1)_C C_1 + (F_N C_2)_C C_1 + (V_N C_1)_C C_1 + (V_N C_2)_C C_1 + (V_N C_3)_C C_1], \quad (\text{B.7})$$

$$\Theta'' = 2(F_N C_1)_{FC} \frac{1}{2} C_1^2 + 2(V_N C_2)_{FC} \frac{1}{2} C_1^2, \quad (\text{B.8})$$

and

$$\Theta_2 = -[(F_N C_1)_{FC} C_2 + (V_N C_2)_{FC} C_2]. \quad (\text{B.9})$$

After adding and subtracting $F_N C_1$ on the left-hand side of eq B.6, we obtain

$$\begin{aligned} \langle \Phi_{ij}^{ab} | [F_N C_1 + (F_N C_2)_C + (F_N C_3)_C + V_N + (V_N C_1)_C + (V_N C_2)_C + (V_N C_3)_C \\ + (V_N C_4)_C + \tilde{\Theta}' + \Theta'' + \Theta_2] | \Phi \rangle = 0, \end{aligned} \quad (\text{B.10})$$

where

$$\tilde{\Theta}' = \Theta' - F_N C_1. \quad (\text{B.11})$$

Using eq B.7, factoring out C_1 , and taking advantage of the already obtained CI equations projected on the singly excited determinants, eq B.5, the contribution from the $\tilde{\Theta}'$ term,

defined by eq B.11, to eq B.10, can be rewritten as follows:

$$\begin{aligned}
\langle \Phi_{ij}^{ab} | \tilde{\Theta}' | \Phi \rangle &= - \langle \Phi_{ij}^{ab} | [F_N C_1 + (F_N C_1)_C C_1 + (F_N C_2)_C C_1 + (V_N C_1)_C C_1 \\
&\quad + (V_N C_2)_C C_1 + (V_N C_3)_C C_1] | \Phi \rangle \\
&= - \langle \Phi_{ij}^{ab} | [F_N + (F_N C_1)_C + (F_N C_2)_C + (V_N C_1)_C + (V_N C_2)_C \\
&\quad + (V_N C_3)_C] C_1 | \Phi \rangle \\
&= -\Delta E^{(\text{CI})} \langle \Phi_{ij}^{ab} | C_1^2 | \Phi \rangle.
\end{aligned} \tag{B.12}$$

At the same time, the contributions from the unlinked Θ'' and Θ_2 terms to eq B.10, after factoring out C_1^2 and C_2 , respectively, and using eq B.4 for the CI correlation energy, become

$$\begin{aligned}
\langle \Phi_{ij}^{ab} | \Theta'' | \Phi \rangle &= \langle \Phi_{ij}^{ab} | [2(F_N C_1)_{FC} \frac{1}{2} C_1^2 + 2(V_N C_2)_{FC} \frac{1}{2} C_1^2] | \Phi \rangle \\
&= \langle \Phi_{ij}^{ab} | [(F_N C_1)_{FC} + (V_N C_2)_{FC}] C_1^2 | \Phi \rangle \\
&= \Delta E^{(\text{CI})} \langle \Phi_{ij}^{ab} | C_1^2 | \Phi \rangle
\end{aligned} \tag{B.13}$$

and

$$\begin{aligned}
\langle \Phi_{ij}^{ab} | \Theta_2 | \Phi \rangle &= - \langle \Phi_{ij}^{ab} | [(F_N C_1)_{FC} C_2 + (V_N C_2)_{FC} C_2] | \Phi \rangle \\
&= - \langle \Phi_{ij}^{ab} | [(F_N C_1)_{FC} + (V_N C_2)_{FC}] C_2 | \Phi \rangle \\
&= -\Delta E^{(\text{CI})} \langle \Phi_{ij}^{ab} | C_2 | \Phi \rangle.
\end{aligned} \tag{B.14}$$

Note that after all of these manipulations the $\tilde{\Theta}'$ and Θ'' contributions to eq B.10, eqs B.12 and B.13, respectively, cancel each other. Thus, after inserting eq B.14 back to eq B.10 and moving the energy-dependent $\Delta E^{(\text{CI})} \langle \Phi_{ij}^{ab} | C_2 | \Phi \rangle$ contribution to the right-hand side of the resulting formula, we arrive at

$$\begin{aligned}
\langle \Phi_{ij}^{ab} | [F_N C_1 + (F_N C_2)_C + (F_N C_3)_C + V_N + (V_N C_1)_C + (V_N C_2)_C \\
+ (V_N C_3)_C + (V_N C_4)_C] | \Phi \rangle &= \Delta E^{(\text{CI})} \langle \Phi_{ij}^{ab} | C_2 | \Phi \rangle,
\end{aligned} \tag{B.15}$$

which is equivalent to eq 22, when expressed in terms of the one- and two-body components of H_N . This completes the proof of the equivalence of eqs 6 and 22 and the diagrammatic derivation of the CI eqs 21–23 from the CC eqs 5–7. The equivalence of eqs 7 and 23 for the correlation energy is an obvious consequence of replacing T_1 and T_2 in eq 7 by the formulas in terms of C_1 and C_2 originating from eq 11, which leads directly to eq B.4 and its analog, eq 23.

References

- (1) Hubbard, J. The description of collective motions in terms of many-body perturbation theory. *Proc. R. Soc. London A* **1957**, *240*, 539–560.
- (2) Hugenholtz, N. M. Perturbation theory of large quantum systems. *Physica* **1957**, *23*, 481–532.
- (3) Coester, F. Bound states of a many-particle system. *Nucl. Phys.* **1958**, *7*, 421–424.
- (4) Čížek, J. On the correlation problem in atomic and molecular systems. Calculation of wavefunction components in Ursell-type expansion using quantum-field theoretical methods. *J. Chem. Phys.* **1966**, *45*, 4256–4266.
- (5) Čížek, J. On the use of the cluster expansion and the technique of diagrams in calculations of correlation effects in atoms and molecules. *Adv. Chem. Phys.* **1969**, *14*, 35–89.
- (6) Paldus, J.; Čížek, J.; Shavitt, I. Correlation problems in atomic and molecular systems. IV. Extended coupled-pair many-electron theory and its application to the BH_3 molecule. *Phys. Rev. A* **1972**, *5*, 50–67.
- (7) Paldus, J.; Li, X. A critical assessment of coupled cluster method in quantum chemistry. *Adv. Chem. Phys.* **1999**, *110*, 1–175.
- (8) Bartlett, R. J.; Musiał, M. Coupled-cluster theory in quantum chemistry. *Rev. Mod. Phys.* **2007**, *79*, 291–352.
- (9) Purvis, G. D., III; Bartlett, R. J. A full coupled-cluster singles and doubles model: The inclusion of disconnected triples. *J. Chem. Phys.* **1982**, *76*, 1910–1918.
- (10) Cullen, J. M.; Zerner, M. C. The linked singles and doubles model: An approximate theory of electron correlation based on the coupled-cluster ansatz. *J. Chem. Phys.* **1982**, *77*, 4088–4109.

- (11) Raghavachari, K.; Trucks, G. W.; Pople, J. A.; Head-Gordon, M. A fifth-order perturbation comparison of electron correlation theories. *Chem. Phys. Lett.* **1989**, *157*, 479–483.
- (12) Piecuch, P.; Zarrabian, S.; Paldus, J.; Čížek, J. Coupled-cluster approaches with an approximate account of triexcitations and the optimized-inner-projection technique. II. Coupled-cluster results for cyclic-polyene model systems. *Phys. Rev. B* **1990**, *42*, 3351–3379.
- (13) Noga, J.; Bartlett, R. J. The full CCSDT model for molecular electronic structure. *J. Chem. Phys.* **1987**, *86*, 7041–7050, **1988**, *89*, 3401 [Erratum].
- (14) Scuseria, G. E.; Schaefer, H. F., III A new implementation of the full CCSDT model for molecular electronic structure. *Chem. Phys. Lett.* **1988**, *152*, 382–386.
- (15) Oliphant, N.; Adamowicz, L. Coupled-cluster method truncated at quadruples. *J. Chem. Phys.* **1991**, *95*, 6645–6651.
- (16) Kucharski, S. A.; Bartlett, R. J. The coupled-cluster single, double, triple, and quadruple excitation method. *J. Chem. Phys.* **1992**, *97*, 4282–4288.
- (17) Podeszwa, R.; Kucharski, S. A.; Stolarczyk, L. Z. Electronic correlation in cyclic polyenes. Performance of coupled-cluster methods with higher excitations. *J. Chem. Phys.* **2002**, *116*, 480–493.
- (18) Degroote, M.; Henderson, T. M.; Zhao, J.; Dukelsky, J.; Scuseria, G. E. Polynomial similarity transformation theory: A smooth interpolation between coupled cluster doubles and projected BCS applied to the reduced BCS Hamiltonian. *Phys. Rev. B* **2016**, *93*, 125124.
- (19) Lyakh, D. I.; Musiał, M.; Lotrich, V. F.; Bartlett, R. J. Multireference nature of chemistry: The coupled-cluster view. *Chem. Rev.* **2012**, *112*, 182–243.

- (20) Evangelista, F. A. Perspective: Multireference coupled cluster theories of dynamical electron correlation. *J. Chem. Phys.* **2018**, *149*, 030901.
- (21) Paldus, J.; Čížek, J.; Takahashi, M. Approximate account of the connected quadruply excited clusters in the coupled-pair many-electron theory. *Phys. Rev. A* **1984**, *30*, 2193–2209.
- (22) Piecuch, P.; Tobiła, R.; Paldus, J. Approximate account of connected quadruply excited clusters in single-reference coupled-cluster theory via cluster analysis of the projected unrestricted Hartree-Fock wave function. *Phys. Rev. A* **1996**, *54*, 1210–1241.
- (23) Paldus, J.; Planelles, J. Valence bond corrected single reference coupled cluster approach I. General formalism. *Theor. Chim. Acta* **1994**, *89*, 13–31.
- (24) Stolarczyk, L. Z. Complete active space coupled-cluster method. Extension of single-reference coupled-cluster method using the CASSCF wavefunction. *Chem. Phys. Lett.* **1994**, *217*, 1–6.
- (25) Peris, G.; Planelles, J.; Paldus, J. Single-reference CCSD approach employing three- and four-body CAS SCF corrections: A preliminary study of a simple model. *Int. J. Quantum Chem.* **1997**, *62*, 137–151.
- (26) Peris, G.; Planelles, J.; Malrieu, J.-P.; Paldus, J. Perturbatively selected CI as an optimal source for externally corrected CCSD. *J. Chem. Phys.* **1999**, *110*, 11708–11716.
- (27) Li, X.; Paldus, J. Reduced multireference CCSD method: An effective approach to quasidegenerate states. *J. Chem. Phys.* **1997**, *107*, 6257–6269.
- (28) Li, X.; Paldus, J. Reduced multireference couple cluster method. II. Application to potential energy surfaces of HF, F₂, and H₂O. *J. Chem. Phys.* **1998**, *108*, 637–648.
- (29) Li, X.; Paldus, J. Reduced multireference coupled cluster method with singles and doubles: Perturbative corrections for triples. *J. Chem. Phys.* **2006**, *124*, 174101.

- (30) Deustua, J. E.; Magoulas, I.; Shen, J.; Piecuch, P. Communication: Approaching exact quantum chemistry by cluster analysis of full configuration interaction quantum Monte Carlo wave functions. *J. Chem. Phys.* **2018**, *149*, 151101.
- (31) Aroeira, G. J. R.; Davis, M. M.; Turney, J. M.; Schaefer, H. F., III Coupled cluster externally corrected by adaptive configuration interaction. *J. Chem. Theory Comput.* **2021**, *17*, 182–190.
- (32) Paldus, J. Externally and internally corrected coupled cluster approaches: An overview. *J. Math. Chem.* **2017**, *55*, 477–502.
- (33) Piecuch, P. Active-space coupled-cluster methods. *Mol. Phys.* **2010**, *108*, 2987–3015.
- (34) Piecuch, P.; Paldus, J. On the solution of coupled-cluster equations in the fully correlated limit of cyclic polyene model. *Int. J. Quantum Chem. Symp.* **1991**, *25*, 9–34.
- (35) Eriksen, J. J.; Anderson, T. A.; Deustua, J. E.; Ghanem, K.; Hait, D.; Hoffmann, M. R.; Lee, S.; Levine, D. S.; Magoulas, I.; Shen, J.; Tubman, N. M.; Whaley, K. B.; Xu, E.; Yao, Y.; Zhang, N.; Alavi, A.; Chan, G. K.-L.; Head-Gordon, M.; Liu, W.; Piecuch, P.; Sharma, S.; Ten-no, S. L.; Umrigar, C. J.; Gauss, J. The ground state electronic energy of benzene. *J. Phys. Chem. Lett.* **2020**, *11*, 8922–8929.
- (36) Xu, E.; Li, S. The externally corrected coupled cluster approach with four- and five-body clusters from the CASSCF wave function. *J. Chem. Phys.* **2015**, *142*, 094119.
- (37) Booth, G. H.; Thom, A. J. W.; Alavi, A. Fermion Monte Carlo without fixed nodes: A game of life, death, and annihilation in Slater determinant space. *J. Chem. Phys.* **2009**, *131*, 054106.
- (38) Cleland, D.; Booth, G. H.; Alavi, A. Communications: Survival of the fittest: Accelerating convergence in full configuration-interaction quantum Monte Carlo. *J. Chem. Phys.* **2010**, *132*, 041103.

- (39) Ghanem, K.; Lozovoi, A. Y.; Alavi, A. Unbiasing the initiator approximation in full configuration interaction quantum Monte Carlo. *J. Chem. Phys.* **2019**, *151*, 224108.
- (40) Ghanem, K.; Guthrie, K.; Alavi, A. The adaptive shift method in full configuration interaction quantum Monte Carlo: Development and applications. *J. Chem. Phys.* **2020**, *153*, 224115.
- (41) Li, X.; Paldus, J. Dissociation of N₂ triple bond: A reduced multireference CCSD study. *Chem. Phys. Lett.* **1998**, *286*, 145–154.
- (42) Li, X.; Paldus, J. Reduced multireference coupled cluster method IV: Open-shell systems. *Mol. Phys.* **2000**, *98*, 1185–1199.
- (43) Li, X.; Paldus, J. Reduced multireference coupled cluster method: Ro-vibrational spectra of N₂. *J. Chem. Phys.* **2000**, *113*, 9966–9977.
- (44) Li, X.; Paldus, J. Full potential energy curve for N₂ by the reduced multireference coupled-cluster method. *J. Chem. Phys.* **2008**, *129*, 054104.
- (45) Li, X.; Gour, J. R.; Paldus, J.; Piecuch, P. On the significance of quadruply excited clusters in coupled-cluster calculations for the low-lying states of BN and C₂. *Chem. Phys. Lett.* **2008**, *461*, 321–326.
- (46) Li, X.; Paldus, J. Electronic structure of organic diradicals: Evaluation of the performance of coupled-cluster methods. *J. Chem. Phys.* **2008**, *129*, 174101.
- (47) Schriber, J. B.; Evangelista, F. A. Communication: An adaptive configuration interaction approach for strongly correlated electrons with tunable accuracy. *J. Chem. Phys.* **2016**, *144*, 161106.
- (48) Schriber, J. B.; Evangelista, F. A. Adaptive configuration interaction for computing challenging electronic excited states with tunable accuracy. *J. Chem. Theory Comput.* **2017**, *13*, 5354–5366.

- (49) Huron, B.; Malrieu, J. P.; Rancurel, P. Iterative perturbation calculations of ground and excited state energies from multiconfigurational zeroth-order wavefunctions. *J. Chem. Phys.* **1973**, *58*, 5745–5759.
- (50) Garniron, Y.; Scemama, A.; Loos, P.-F.; Caffarel, M. Hybrid stochastic-deterministic calculation of the second-order perturbative contribution of multireference perturbation theory. *J. Chem. Phys.* **2017**, *147*, 034101.
- (51) Garniron, Y.; Applencourt, T.; Gasperich, K.; Benali, A.; Ferté, A.; Paquier, J.; Pradines, B.; Assaraf, R.; Reinhardt, P.; Toulouse, J.; Barbaresco, P.; Renon, N.; David, G.; Malrieu, J.-P.; Véril, M.; Caffarel, M.; Loos, P.-F.; Giner, E.; Scemama, A. Quantum Package 2.0: An open-source determinant-driven suite of programs. *J. Chem. Theory Comput.* **2019**, *15*, 3591–3609.
- (52) Whitten, J. L.; Hackmeyer, M. Configuration interaction studies of ground and excited states of polyatomic molecules. I. The CI formulation and studies of formaldehyde. *J. Chem. Phys.* **1969**, *51*, 5584–5596.
- (53) Bender, C. F.; Davidson, E. R. Studies in configuration interaction: The first-row diatomic hydrides. *Phys. Rev.* **1969**, *183*, 23–30.
- (54) Buenker, R. J.; Peyerimhoff, S. D. Individualized configuration selection in CI calculations with subsequent energy extrapolation. *Theor. Chim. Acta* **1974**, *35*, 33–58.
- (55) Tubman, N. M.; Lee, J.; Takeshita, T. Y.; Head-Gordon, M.; Whaley, K. B. A deterministic alternative to the full configuration interaction quantum Monte Carlo method. *J. Chem. Phys.* **2016**, *145*, 044112.
- (56) Tubman, N. M.; Freeman, C. D.; Levine, D. S.; Hait, D.; Head-Gordon, M.; Whaley, K. B. Modern approaches to exact diagonalization and selected configuration interaction with the adaptive sampling CI method. *J. Chem. Theory Comput.* **2020**, *16*, 2139–2159.

- (57) Liu, W.; Hoffmann, M. R. iCI: Iterative CI toward full CI. *J. Chem. Theory Comput.* **2016**, *12*, 1169–1178, **2016**, *12*, 3000 [Erratum].
- (58) Zhang, N.; Liu, W.; Hoffmann, M. R. Iterative configuration interaction with selection. *J. Chem. Theory Comput.* **2020**, *16*, 2296–2316.
- (59) Holmes, A. A.; Tubman, N. M.; Umrigar, C. J. Heat-bath configuration interaction: An efficient selected configuration interaction algorithm inspired by heat-bath sampling. *J. Chem. Theory Comput.* **2016**, *12*, 3674–3680.
- (60) Sharma, S.; Holmes, A. A.; Jeanmairet, G.; Alavi, A.; Umrigar, C. J. Semistochastic heat-bath configuration interaction method: Selected configuration interaction with semistochastic perturbation theory. *J. Chem. Theory Comput.* **2017**, *13*, 1595–1604.
- (61) Li, J.; Otten, M.; Holmes, A. A.; Sharma, S.; Umrigar, C. J. Fast semistochastic heat-bath configuration interaction. *J. Chem. Phys.* **2018**, *149*, 214110.
- (62) Loos, P.-F.; Damour, Y.; Scemama, A. The performance of CIPSI on the ground state electronic energy of benzene. *J. Chem. Phys.* **2020**, *153*, 176101.
- (63) Paldus, J. In *Methods in Computational Molecular Physics*; Wilson, S., Diercksen, G. H. F., Eds.; NATO Advanced Study Institute, Series B: Physics; Plenum: New York, 1992; Vol. 293; pp 99–194.
- (64) Piecuch, P.; Kowalski, K. In *Computational Chemistry: Reviews of Current Trends*; Leszczyński, J., Ed.; World Scientific: Singapore, 2000; Vol. 5; pp 1–104.
- (65) Kowalski, K.; Piecuch, P. The method of moments of coupled-cluster equations and the renormalized CCSD[T], CCSD(T), CCSD(TQ), and CCSDT(Q) approaches. *J. Chem. Phys.* **2000**, *113*, 18–35.

- (66) Piecuch, P.; Kowalski, K.; Pimienta, I. S. O.; Mcguire, M. J. Recent advances in electronic structure theory: Method of moments of coupled-cluster equations and renormalized coupled-cluster approaches. *Int. Rev. Phys. Chem.* **2002**, *21*, 527–655.
- (67) Dunning, T. H., Jr. Gaussian basis sets for use in correlated molecular calculations. I. The atoms boron through neon and hydrogen. *J. Chem. Phys.* **1989**, *90*, 1007–1023.
- (68) Olsen, J.; Jørgensen, P.; Koch, H.; Balkova, A.; Bartlett, R. J. Full configuration–interaction and state of the art correlation calculations on water in a valence double-zeta basis with polarization functions. *J. Chem. Phys.* **1996**, *104*, 8007–8015.
- (69) Bauman, N. P.; Shen, J.; Piecuch, P. Combining active-space coupled-cluster approaches with moment energy corrections via the CC($P;Q$) methodology: Connected quadruple excitations. *Mol. Phys.* **2017**, *115*, 2860–2891.
- (70) Deustua, J. E.; Shen, J.; Piecuch, P. High-level coupled-cluster energetics by Monte Carlo sampling and moment expansions: Further details and comparisons. *J. Chem. Phys.*, submitted (2021).
- (71) Schmidt, M. W.; Baldrige, K. K.; Boatz, J. A.; Elbert, S. T.; Gordon, M. S.; Jensen, J. H.; Koseki, S.; Matsunaga, N.; Nguyen, K. A.; Su, S.; Windus, T. L.; Dupuis, M.; Montgomery, Jr., J. A. General atomic and molecular electronic structure system. *J. Comput. Chem.* **1993**, *14*, 1347–1363.
- (72) Barca, G. M. J.; Bertoni, C.; Carrington, L.; Datta, D.; De Silva, N.; Deustua, J. E.; Fedorov, D. G.; Gour, J. R.; Gunina, A. O.; Guidez, E.; Harville, T.; Irle, S.; Ivanic, J.; Kowalski, K.; Leang, S. S.; Li, H.; Li, W.; Lutz, J. J.; Magoulas, I.; Mato, J.; Mironov, V.; Nakata, H.; Pham, B. Q.; Piecuch, P.; Poole, D.; Pruitt, S. R.; Rendell, A. P.; Roskop, L. B.; Ruedenberg, K.; Sattasathuchana, T.; Schmidt, M. W.; Shen, J.; Slipchenko, L.; Sosonkina, M.; Sundriyal, V.; Tiwari, A.; Galvez Vallejo, J. L.; Westheimer, B.; Włoch, M.; Xu, P.; Zahariev, F.; Gordon, M. S. Recent developments

- in the general atomic and molecular electronic structure system. *J. Chem. Phys.* **2020**, *152*, 154102.
- (73) Ivanic, J. Direct configuration interaction and multiconfigurational self-consistent-field method for multiple active spaces with variable occupations. I. Method. *J. Chem. Phys.* **2003**, *119*, 9364–9376.
- (74) Ivanic, J. Direct configuration interaction and multiconfigurational self-consistent-field method for multiple active spaces with variable occupations. II. Application to oxoMn(salen) and N₂O₄. *J. Chem. Phys.* **2003**, *119*, 9377–9385.
- (75) Ivanic, J.; Ruedenberg, K. Identification of deadwood in configuration spaces through general direct configuration interaction. *Theor. Chem. Acc.* **2001**, *106*, 339–351.
- (76) Shen, J.; Piecuch, P. Biorthogonal moment expansions in coupled-cluster theory: Review of key concepts and merging the renormalized and active-space coupled-cluster methods. *Chem. Phys.* **2012**, *401*, 180–202.
- (77) Shen, J.; Piecuch, P. Combining active-space coupled-cluster methods with moment energy corrections via the CC(*P*;*Q*) methodology, with benchmark calculations for biradical transition states. *J. Chem. Phys.* **2012**, *136*, 144104.
- (78) Deustua, J. E.; Shen, J.; Piecuch, P. Converging high-level coupled-cluster energetics by Monte Carlo sampling and moment expansions. *Phys. Rev. Lett.* **2017**, *119*, 223003.
- (79) Yuwono, S. H.; Chakraborty, A.; Deustua, J. E.; Shen, J.; Piecuch, P. Accelerating convergence of equation-of-motion coupled-cluster computations using the semi-stochastic CC(*P*;*Q*) formalism. *Mol. Phys.* **2020**, *118*, e1817592.
- (80) Piecuch, P.; Włoch, M. Renormalized coupled-cluster methods exploiting left eigenstates of the similarity-transformed Hamiltonian. *J. Chem. Phys.* **2005**, *123*, 224105.

- (81) Piecuch, P.; Włoch, M.; Gour, J. R.; Kinal, A. Single-reference, size-extensive, non-iterative coupled-cluster approaches to bond breaking and biradicals. *Chem. Phys. Lett.* **2006**, *418*, 467–474.
- (82) Magoulas, I.; Bauman, N. P.; Shen, J.; Piecuch, P. Application of the CC($P;Q$) hierarchy of coupled-cluster methods to the beryllium dimer. *J. Phys. Chem. A* **2018**, *122*, 1350–1368.
- (83) Yuwono, S. H.; Magoulas, I.; Shen, J.; Piecuch, P. Application of the coupled-cluster CC($P;Q$) approaches to the magnesium dimer. *Mol. Phys.* **2019**, *117*, 1486–1506.

Table 1: A comparison of the energies resulting from the various CI and CC all-electron calculations for the H₂O molecule, as described by the cc-pVDZ basis set,⁶⁷ at the equilibrium and two displaced geometries in which both O–H bonds are stretched by factors of 2 and 3.^a

wave function	CI/CC energy	ec-CC energy	
		I	II
	$R = R_e$		
CISD	12.023	12.023	3.744 ^b
CISDT	9.043	9.043	0.455
CISDTQ	0.327	0.327	0.327
CISDTQP	0.139	0.139	0.139
CISDTQPH	0.003	0.003	0.003
CCSD ^c	3.744	3.744	3.744
CCSDT ^c	0.493	0.493	0.493
CCSDTQ ^c	0.019	0.019	0.019
FCI ^d	-76.241860		
	$R = 2R_e$		
CISD	72.017	72.017	22.034 ^b
CISDT	56.096	56.096	2.920
CISDTQ	5.819	5.819	5.819
CISDTQP	2.236	2.236	2.236
CISDTQPH	0.059	0.059	0.059
CCSD ^c	22.034	22.034	22.034
CCSDT ^c	-1.403	-1.403	-1.403
CCSDTQ ^c	0.032	0.032	0.032
FCI ^d	-75.951667		
	$R = 3R_e$		
CISD	164.949	164.949	10.849 ^b
CISDT	118.119	118.119	-77.317
CISDTQ	16.150	16.150	16.150
CISDTQP	6.432	6.432	6.432
CISDTQPH	0.159	0.159	0.159
CCSD ^c	10.849	10.849	10.849
CCSDT ^c	-40.126	-40.126	-40.126
CCSDTQ ^c	-4.733	-4.733	-4.733
FCI ^d	-75.911946		

^a The equilibrium geometry, $R = R_e$, and the geometries that represent a simultaneous stretching of both O–H bonds by factors of 2 and 3 without changing the $\angle(\text{H–O–H})$ angle were taken from ref 68. Unless otherwise stated, all energies are errors relative to FCI in millihartree. ^b Equivalent to CCSD. ^c Taken from ref 69. ^d Total FCI energy in hartree.

Table 2: Convergence of the energies resulting from the all-electron CIPSI calculations initiated from the RHF wave function and the corresponding CIPSI-based ec-CC energies toward FCI for the H₂O molecule, as described by the cc-pVDZ basis set,⁶⁷ at the equilibrium and two displaced geometries in which both O–H bonds are stretched by factors of 2 and 3.^a

N _{det(in)} / N _{det(out)}	%S ^b	%D ^b	%T ^b	%Q ^b	CIPSI ^c		ec-CC ^c	
					E_{var}	$E_{\text{var}} + \Delta E^{(2)}$	I	II
	$R = R_e$							
1 / 1	0	0	0	0	217.822 ^d	-42.098	3.744 ^e	0.344 ^f
1,000 / 1,299	15.2	37.9	0	0.0	21.589	-0.109	11.019	3.637
5,000 / 5,216	51.5	73.8	1.0	0.2	8.445	0.098	8.123	2.455
10,000 / 10,448	60.6	80.4	3.1	0.4	6.587	0.184	6.441	1.887
50,000 / 83,762	93.9	94.7	22.1	4.9	2.612	0.089	2.610	0.626
100,000 / 167,425	93.9	97.8	34.5	10.0	1.743	0.064	1.742	0.410
500,000 / 665,840	100	99.7	69.0	31.9	0.435	0.008	0.435	0.120
1,000,000 / 1,308,003	100	99.9	82.5	45.6	0.229	0.004	0.229	0.069
	$R = 2R_e$							
1 / 1	0	0	0	0	363.956 ^d	-180.621	22.034 ^e	-0.548 ^f
1,000 / 1,399	36.4	18.1	0.3	0.0	34.996	1.884	26.505	-0.454
5,000 / 5,664	54.5	43.1	1.8	0.2	13.817	0.605	12.707	0.226
10,000 / 11,350	57.6	55.6	3.6	0.4	9.011	0.375	8.653	0.321
50,000 / 90,880	93.9	85.3	21.6	3.7	2.436	0.084	2.429	0.515
100,000 / 181,579	100	91.6	31.7	6.8	1.418	0.046	1.417	0.356
500,000 / 718,316	100	97.7	59.6	21.4	0.273	0.009	0.273	0.138
1,000,000 / 1,390,678	100	99.3	73.2	31.9	0.137	0.003	0.137	0.072
	$R = 3R_e$							
1 / 1	0	0	0	0	567.554 ^d	-227.583	10.849 ^e	-40.556 ^f
1,000 / 1,437	30.3	8.8	0.3	0.1	28.755	1.010	22.107	-1.934
5,000 / 5,793	39.4	21.4	1.8	0.2	9.919	0.337	9.546	1.507
10,000 / 11,603	54.5	28.6	3.5	0.4	5.258	0.157	5.093	0.699
50,000 / 92,707	87.9	70.8	14.9	2.5	0.906	0.031	0.902	0.358
100,000 / 184,903	90.9	78.5	22.7	4.4	0.483	0.011	0.483	0.228
500,000 / 703,445	97.0	89.3	46.0	13.5	0.071	-0.001	0.071	0.050
1,000,000 / 1,215,321	97.0	92.8	56.3	19.5	0.029	-0.001	0.029	0.017

^a The equilibrium geometry, $R = R_e$, and the geometries that represent a simultaneous stretching of both O–H bonds by factors of 2 and 3 without changing the $\angle(\text{H-O-H})$ angle were taken from ref 68. ^b %S, %D, %T, and %Q are, respectively, the percentages of the singly, doubly, triply, and quadruply excited $S_z = 0$ determinants of A_1 symmetry captured during the CIPSI computations. ^c Errors relative to FCI in millihartree (see Table 1 for the FCI energies). ^d Equivalent to RHF. ^e Equivalent to CCSD. ^f Equivalent to CR-CC(2,3).

Table 3: Convergence of the energies resulting from the all-electron CIPSI calculations initiated from the CISD wave function and the corresponding CIPSI-based ec-CC energies toward FCI for the H₂O molecule, as described by the cc-pVDZ basis set,⁶⁷ at $R = 2R_e$.^a

N _{det(in)} / N _{det(out)}	%S ^b	%D ^b	%T ^b	%Q ^b	CIPSI ^c		ec-CC ^c		
					E_{var}	$E_{\text{var}} + \Delta E^{(2)}$	I	II	II ₃
5,000 / 6,887	100	100	1.5	0.2	20.034	1.755	20.034	9.408	3.390
10,000 / 13,788	100	100	4.3	0.5	10.053	0.464	10.053	3.085	0.374
50,000 / 55,194	100	100	14.8	2.2	3.422	0.125	3.422	0.920	0.434
100,000 / 110,334	100	100	23.6	4.5	2.472	0.076	2.472	0.638	0.410
500,000 / 793,987	100	100	61.5	22.9	0.239	0.009	0.239	0.117	0.109
1,000,000 / 1,476,373	100	100	74.1	33.1	0.119	0.004	0.119	0.063	0.062

^a The geometry representing a simultaneous stretching of both O–H bonds by a factor of 2 without changing the $\angle(\text{H–O–H})$ angle was taken from ref 68. For this problem, the CISD wave function contains 3,416 $S_z = 0$ determinants of A_1 symmetry. ^b %S, %D, %T, and %Q are, respectively, the percentages of the singly, doubly, triply, and quadruply excited $S_z = 0$ determinants of A_1 symmetry captured during the CIPSI computations.

^c Errors relative to FCI in millihartree (for the FCI energy at $R = 2R_e$, see Table 1).

$$\begin{aligned}
F_N &\rightarrow F_N \\
(F_N T_1)_C &\rightarrow (F_N C_1)_C \\
(F_N T_2)_C &\rightarrow (F_N C_2)_C - \cancel{(F_N \frac{1}{2} C_1^2)_C} - (F_N C_1)_{FC} C_1 \\
(F_N \frac{1}{2} T_1^2)_C &\rightarrow \cancel{(F_N \frac{1}{2} C_1^2)_C} \\
(V_N T_1)_C &\rightarrow (V_N C_1)_C \\
(V_N T_2)_C &\rightarrow (V_N C_2)_C - \cancel{(V_N \frac{1}{2} C_1^2)_C} \\
(V_N \frac{1}{2} T_1^2)_C &\rightarrow \cancel{(V_N \frac{1}{2} C_1^2)_C} \\
(V_N T_3)_C &\rightarrow (V_N C_3)_C - \cancel{(V_N C_1 C_2)_C} - (V_N C_2)_{FC} C_1 + 2 \cancel{(V_N \frac{1}{3!} C_1^3)_C} + 2 \cancel{(V_N \frac{1}{2} C_1^2)_{FC} C_1} \\
(V_N T_1 T_2)_C &\rightarrow \cancel{(V_N C_1 C_2)_C} - 3 \cancel{(V_N \frac{1}{3!} C_1^3)_C} - 2 \cancel{(V_N \frac{1}{2} C_1^2)_{FC} C_1} \\
(V_N \frac{1}{3!} T_1^3)_C &\rightarrow \cancel{(V_N \frac{1}{3!} C_1^3)_C}
\end{aligned}$$

Chart B.1: The correspondence between the various $(H_N e^T)_C$ contributions to the CC equations projected on the singly excited determinants, eq 5, and their counterparts resulting from the application of eq 11. The unlinked terms in which the fully connected operator products $(F_N C_1)_{FC}$ and $(V_N C_2)_{FC}$ that contribute to the correlation energy multiply C_1 , resulting in eq B.2, are highlighted in red.

$$\begin{aligned}
(F_N T_2)_C &\rightarrow (F_N C_2)_C - (F_N C_1)_C C_1 \\
(F_N T_3)_C &\rightarrow (F_N C_3)_C - \overline{(F_N C_1 C_2)_C} - (F_N C_2)_C C_1 - (F_N C_1)_{FC} C_2 + \overline{2(F_N \frac{1}{2} C_1^2)_C C_1} \\
&\quad + 2(F_N C_1)_{FC} \frac{1}{2} C_1^2 \\
(F_N T_1 T_2)_C &\rightarrow \overline{(F_N C_1 C_2)_C} - \overline{2(F_N \frac{1}{2} C_1^2)_C C_1} \\
V_N &\rightarrow V_N \\
(V_N T_1)_C &\rightarrow (V_N C_1)_C \\
(V_N T_2)_C &\rightarrow (V_N C_2)_C - \overline{(V_N \frac{1}{2} C_1^2)_C} - (V_N C_1)_C C_1 \\
(V_N \frac{1}{2} T_1^2)_C &\rightarrow \overline{(V_N \frac{1}{2} C_1^2)_C} \\
(V_N T_3)_C &\rightarrow (V_N C_3)_C - \overline{(V_N C_1 C_2)_C} - (V_N C_2)_C C_1 + \overline{2(V_N \frac{1}{3!} C_1^3)_C} + \overline{2(V_N \frac{1}{2} C_1^2)_C C_1} \\
(V_N T_1 T_2)_C &\rightarrow \overline{(V_N C_1 C_2)_C} - \overline{3(V_N \frac{1}{3!} C_1^3)_C} - \overline{2(V_N \frac{1}{2} C_1^2)_C C_1} \\
(V_N \frac{1}{3!} T_1^3)_C &\rightarrow \overline{(V_N \frac{1}{3!} C_1^3)_C} \\
(V_N T_4)_C &\rightarrow (V_N C_4)_C - \overline{(V_N C_1 C_3)_C} - (V_N C_3)_C C_1 - \overline{(V_N \frac{1}{2} C_2^2)_C} - (V_N C_2)_{FC} C_2 \\
&\quad + \overline{2(V_N \frac{1}{2} C_1^2 C_2)_C} + 2(V_N C_2)_{FC} \frac{1}{2} C_1^2 + \overline{2(V_N \frac{1}{2} C_1^2)_{FC} C_2} + \overline{2(V_N C_1 C_2)_C C_1} \\
&\quad - \overline{6(V_N \frac{1}{4!} C_1^4)_C} - \overline{6(V_N \frac{1}{3!} C_1^3)_C C_1} - \overline{6(V_N \frac{1}{2} C_1^2)_{FC} \frac{1}{2} C_1^2} \\
(V_N T_1 T_3)_C &\rightarrow \overline{(V_N C_1 C_3)_C} - \overline{2(V_N \frac{1}{2} C_1^2 C_2)_C} - \overline{2(V_N \frac{1}{2} C_1^2)_{FC} C_2} - \overline{(V_N C_1 C_2)_C C_1} \\
&\quad + \overline{8(V_N \frac{1}{4!} C_1^4)_C} + \overline{6(V_N \frac{1}{3!} C_1^3)_C C_1} + \overline{4(V_N \frac{1}{2} C_1^2)_{FC} \frac{1}{2} C_1^2} \\
(V_N \frac{1}{2} T_2^2)_C &\rightarrow \overline{(V_N \frac{1}{2} C_2^2)_C} - \overline{(V_N \frac{1}{2} C_1^2 C_2)_C} - \overline{(V_N C_1 C_2)_C C_1} + \overline{3(V_N \frac{1}{4!} C_1^4)_C} \\
&\quad + \overline{3(V_N \frac{1}{3!} C_1^3)_C C_1} + \overline{2(V_N \frac{1}{2} C_1^2)_{FC} \frac{1}{2} C_1^2} \\
(V_N \frac{1}{2} T_1^2 T_2)_C &\rightarrow \overline{(V_N \frac{1}{2} C_1^2 C_2)_C} - \overline{6(V_N \frac{1}{4!} C_1^4)_C} - \overline{3(V_N \frac{1}{3!} C_1^3)_C C_1} \\
(V_N \frac{1}{4!} T_1^4)_C &\rightarrow \overline{(V_N \frac{1}{4!} C_1^4)_C}
\end{aligned}$$

Chart B.2: The correspondence between the various $(H_N e^T)_C$ contributions to the CC equations projected on the doubly excited determinants, eq 6, and their counterparts resulting from the application of eq 11. The unlinked terms in which the fully connected operator products $(F_N C_1)_{FC}$ and $(V_N C_2)_{FC}$ that contribute to the correlation energy multiply C_2 , resulting in eq B.9, are highlighted in red. The unlinked terms in which the fully connected operator products $(F_N C_1)_{FC}$ and $(V_N C_2)_{FC}$ that contribute to the correlation energy multiply $\frac{1}{2} C_1^2$, resulting in eq B.8, are highlighted in green. The disconnected terms in which the $(F_N C_1)_C$, $(F_N C_2)_C$, $(V_N C_1)_C$, $(V_N C_2)_C$, and $(V_N C_3)_C$ connected operator products multiply C_1 , resulting in eq B.7, are highlighted in blue.

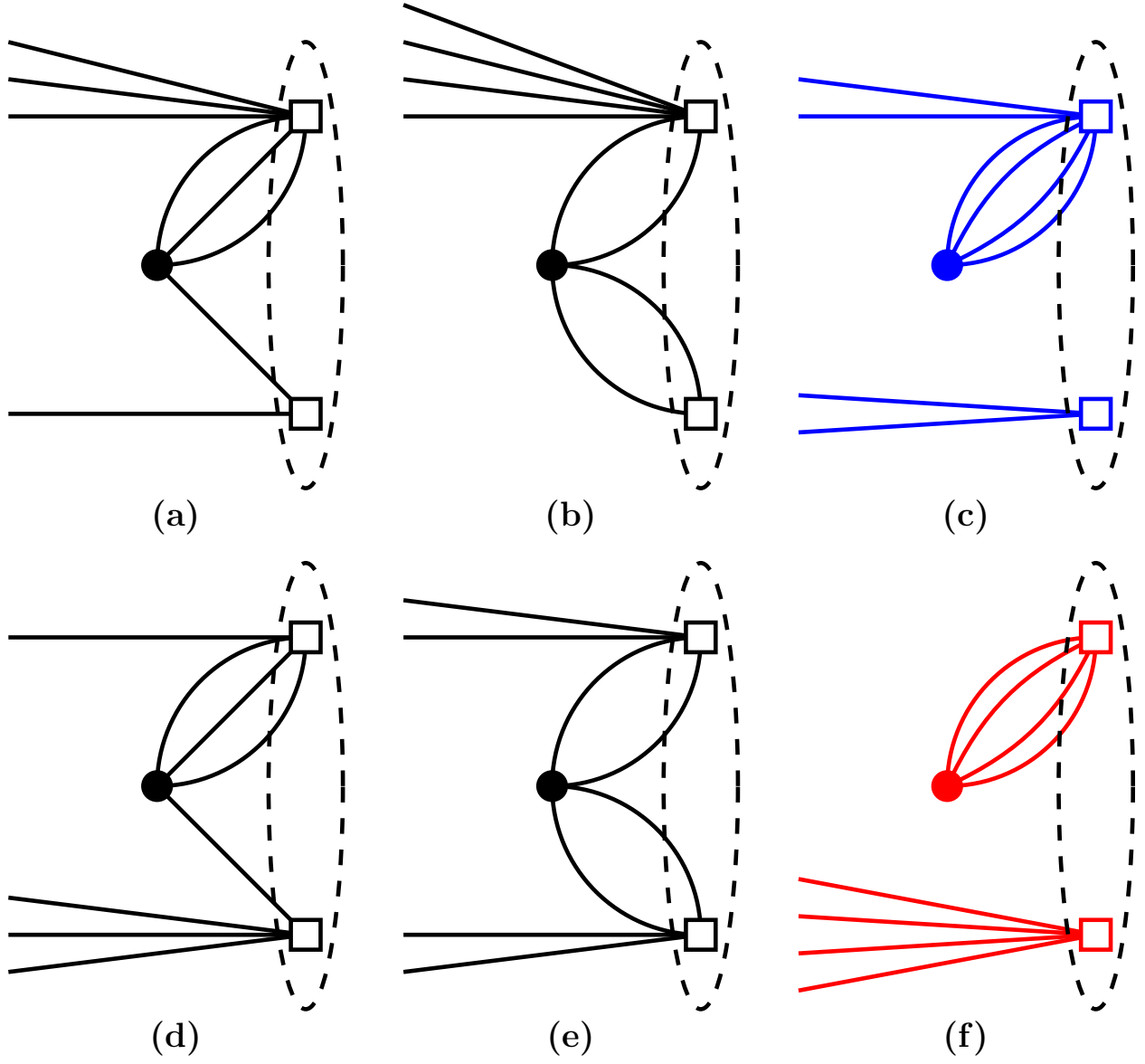


Figure B.1: Hugenholtz diagrammatic representation of the $V_N C_1 C_3$ ((a)–(c)) and $\frac{1}{2} V_N C_2^2$ ((d)–(f)) contributions to $\langle \Phi_{ij}^{ab} | (V_N T_4)_C | \Phi \rangle$ resulting from the application of eq 11 and corresponding to the second through fifth expressions contributing to $(V_N T_4)_C$ in Chart B.2. The solid circle represents the V_N vertex and the open squares with two, four, and six fermion lines designate the C_1 , C_2 , and C_3 operators, respectively. The dashed oval highlights the T_4 operator in $\langle \Phi_{ij}^{ab} | (V_N T_4)_C | \Phi \rangle$. Consistent with Chart B.2, diagram (c), which corresponds to the disconnected $(V_N C_3)_C C_1$ contribution to $\langle \Phi_{ij}^{ab} | (V_N T_4)_C | \Phi \rangle$ (the third term contributing to $(V_N T_4)_C$ in Chart B.2) is highlighted in blue. Diagram (f), which represents the unlinked $(V_N C_2)_{FC} C_2$ contribution to $\langle \Phi_{ij}^{ab} | (V_N T_4)_C | \Phi \rangle$ (the fifth term contributing to $(V_N T_4)_C$ in Chart B.2) is highlighted in red.